1 **Short title**: GWAS of Arabidopsis phosphate starvation tolerance

2 **Corresponding author details:**

3 Dr. Ricarda Jost

4 Department of Animal, Plant and Soil Science

5 La Trobe Institute for Agriculture and Food (LIAF)

6 School of Life Sciences

7 La Trobe University

8 5 Ring Road

9 Bundoora (Melbourne)

10 VIC 3083, Australia

11 Ph.: +61 (0)3 9032 7490

12 Email: r.jost@latrobe.edu.au

13 **Title:**

14 **Diverse phosphate and auxin transport loci distinguish phosphate tolerant from sensitive**

15 **Arabidopsis accessions**

16 **Authors:** Changyu Yi[1], Xinchao Wang[2], Qian Chen[1], Damien L. Callahan[3], Alexandre Fournier-

17 Level[4], James Whelan[1], Ricarda Jost[1]

18 [1] Department of Animal, Plant and Soil Sciences and La Trobe Institute for Agriculture and Food

19 (LIAF), ARC Centre of Excellence in Plant Energy Biology, School of Life Sciences, La Trobe

20 University, Bundoora, Victoria, Australia

21 [2] Key Laboratory of Tea Biology and Resources Utilization, Ministry of Agriculture and Rural Affairs,

22 Tea Research Institute, Chinese Academy of Agricultural Sciences, Hangzhou, China

23 [3] Centre for Chemistry and Biotechnology, School of Life and Environmental Sciences, Deakin

24 University (Burwood Campus), Burwood, Victoria, Australia

25 [4] School of BioSciences, The University of Melbourne, Victoria, Australia

The author responsible for distribution of materials integral to the findings presented in this article in accordance with the policy described in the Instructions for Authors (https://academic.oup.com/plphys/pages/General-Instructions) is James Whelan.

One-Sentence Summary:

A series of insertion/deletion nucleotide polymorphisms at *PHOSPHATE TRANSPORTER1* and *PIN-LIKES7* loci confer natural variation in low phosphate tolerance in 200 Arabidopsis accessions.

Footnotes:

[1] Author contributions: R.J. and J.W. conceived the project. C.Y., X.W. and Q.C. characterized the phosphate starvation response of accessions. D.C. conducted the ICP-MS analyses. C.Y. carried out phosphate and anthocyanin assays, performed GWAS analyses, genotyped T-DNA mutants, generated transgenic germplasm and characterized lines on a molecular and physiological level. C.Y., A.F.-L., J.W. and R.J. interpreted results and drafted the manuscript. All authors reviewed the article.

[*] Corresponding author: Ricarda Jost, e-mail: r.jost@latrobe.edu.au

Abstract

Phosphorus is an essential element for plant growth often limiting agroecosystems. To identify genetic determinants of performance under variable phosphate supply, we conducted genome-wide-association studies on five highly predictive phosphate starvation response traits in 200 Arabidopsis (*Arabidopsis thaliana*) accessions. Phosphate concentration in phosphate-limited organs had the strongest, and primary root length had the weakest genetic component. Of 70 trait-associated candidate genes, 17 responded to phosphate withdrawal. The *PHOSPHATE TRANSPORTER1* gene cluster on chromosome 5 comprised *PHT1;1*, *PHT1;2* and *PHT1;3* with known impact on phosphorus status. A second locus featured uncharacterized endomembrane-associated auxin efflux carrier encoding *PIN-LIKES7* (*PILS7*) which was more strongly suppressed in phosphate-limited roots of phosphate-starvation sensitive accessions. In the Col-0 background, phosphate uptake and organ growth were impaired in both phosphate-limited *pht1;1* and two *pils7* T-DNA insertion mutants, while phosphate-limited *pht1;2* had higher biomass and *pht1;3* was indistinguishable from wild type. Copy number variation at the *PHT1* locus with loss of the *PHT1;3* gene and smaller scale deletions in *PHT1;1* and *PHT1;2* predicted to alter both protein structure and function suggest diversification of *PHT1* is a key driver for adaptation to phosphorus limitation. Haplogroup analysis revealed a phosphorylation site in the protein encoded by the *PILS7* allele from stress-sensitive accessions as well as additional auxin-responsive elements in the promoter of the 'stress tolerant' allele. The former allele's inability to complement the *pils7-1* mutant in the Col-0 background implies the presence of a kinase signaling loop controlling PILS7 activity in accessions from phosphorus-rich environments, while survival in phosphorus-poor environments requires fine-tuning of stress-responsive root auxin signaling.

Introduction

Phosphorus (P) is an essential macronutrient for plant growth and development. However, in most soils, the concentration of Pi is limiting due to its low solubility and mobility (Raghothama, 1999). Pi deficiency commonly impairs plant growth and affects about 70% of cultivated land globally (Cakmak, 2002; Hinsinger, 2001; López-Arredondo et al., 2014). Thus, P-containing chemical fertilizers are essential to sustain sufficient plant growth, as well as high grain quality and yield in most agroecosystems. Plants have evolved an array of strategies to cope with variable Pi environments, including remodeling of root system architecture (RSA) and metabolic adjustments (Bhosale et al., 2018; Plaxton & Tran, 2011; Shahzad & Amtmann, 2017). Auxin plays an important role in altering root system architecture. Application of auxin mimics the root's response to low Pi supply, with a shorter primary root, and increased lateral root and root hair elongation (Bates & Lynch, 1996; Nacry et al., 2005). This phenotype was abolished in the auxin signaling mutants *auxin resistant (axr)1-7*, *axr2-1* and *axr4-1*, *auxin response factor (arf)7*, *arf19* and *transport inhibitor response (tir)1* (Huang et al., 2018; Nacry et al., 2005; Perez-Torres et al., 2008). Plants grown under P-limiting conditions not only accumulate more auxin in roots but are also more responsive to auxin (López-Bucio et al., 2002; Nacry et al., 2005; Perez-Torres et al., 2008).

The molecular mechanisms by which plants respond to Pi limitation are well studied. They consist of MYB transcription factor PHOSPHATE STARVATION RESPONSE1 (PHR1), microRNA *MIR399*, E2 ubiquitin conjugase PHOSPHATE2 (PHO2), Pi exporter PHOSPHATE1 (PHO1) and the PHOSPHATE TRANSPORTER1 (PHT1) family – often referred to as the PHO regulon (Aung et al., 2006; Hamburger et al., 2002; Muchhal et al., 1996; Rubio et al., 2001). Auxin affects Pi starvation signaling by regulating the expression of *PHR1*, which is the transcriptional master regulator of phosphate starvation response (PSR) (Huang et al., 2018). Exogenous auxin application induces *PHR1* expression while auxin transport inhibitors suppress it. Phosphate transporters are responsible for Pi acquisition from the environment and translocation between organs, cell types or organelles. In Arabidopsis (*Arabidopsis thaliana*), nine plasma membrane located PHT1 family members have been characterized, and at least eight of them are expressed in P-limited roots (Mudge et al., 2002; Shin et al., 2004). *PHT1;1*, *PHT1;2*, *PHT1;3* and *PHT1;6* are

4

94   collocated in a gene cluster on chromosome 5 indicating a series of recent gene duplication events

95   (Ayadi et al., 2015). Amongst *PHT1* genes, *PHT1;1* shows the highest expression in P-replete

96   organs, suggesting an important role in bulk Pi uptake. The *pht1;1* mutant shows a 60% reduction

97   of Pi uptake by P-replete roots. Compared to *PHT1;1*, both *PHT1;2* and *PHT1;3* have lower

98   transcript abundance in Pi-rich media but are highly transcribed under Pi starvation (Shin et al.,

99   2004). PHT1;2 and PHT1;3 together contribute about 30% of the Pi uptake in P-limited roots, while

100   PHT1;1 contributes between 15 to 20% (Ayadi et al., 2015).

101   Genome-Wide Association Studies (GWAS) are a powerful tool for identifying genetic

102   variants associated with phenotypic traits. Several GWAS have investigated traits related to plant

103   nutrition (Bouain et al., 2019; Jia et al., 2019; Kawa et al., 2016; Kisko et al., 2018; Rosas et al.,

104   2013; Satbhai et al., 2017). *PHO1* was associated with root plasticity in heterogeneous

105   environments, impacting the distribution of lateral roots along the primary axis (Rosas et al., 2013).

106   Given the importance of the PHO regulon in regulating Pi acquisition and use in the *A. thaliana*

107   reference accession Col-0, it is quite surprising that no natural genetic variation in PHT1 or PHO1

108   transporters has been directly associated with adaptation to variable P environments thus far.

109   In this study, we investigate the genetic basis of the response to changes in Pi availability

110   among 200 highly diverse ecotypes of the model plant *Arabidopsis thaliana*. Focusing on

111   physiological (organ biomass and primary root length) and metabolic traits (organ Pi, shoot

112   anthocyanin and shoot elemental composition), we test the expectation that variation in PSR is

113   primarily mediated by allelic variation at transporter-encoding loci. We leverage the power of

114   GWAS combined with haplogroup structure analysis and functional validation to establish *PHT1*

115   and *PILS7* as important loci underlying natural variation in low phosphate tolerance.

116   **Results**

117   ***Arabidopsis thaliana* accessions display highly diverse responses to Pi withdrawal**

118   The accessions used in this study were selected based on a previous study (Li et al., 2010)

119   to minimize genetic redundancy and family relatedness of accessions and to ensure maximum

120   genetic diversity within the population (Supplemental Table 1). We first assessed the impact of

varying Pi supply on critical growth parameters using developmentally synchronized seedlings

(Materials and Methods, Supplemental Figure 1). We observed reductions in organ biomass, organ

Pi concentration, and primary root growth as well as anthocyanin accumulation in P-limited shoots

(Figure 1, Supplemental Tables 2 and 3) and altered shoot elemental composition (Supplemental

Figure 2A, Supplemental Table 2). Within these general trends, accessions showed large

qualitative and quantitative differences in the degree of PSR (Figure 1, Supplemental Tables 2 and

3). For instance, on average, Pi withdrawal resulted in a 42% reduction of shoot fresh weight, while

it only conferred a 12% reduction of root fresh weight. Pi concentrations in P-limited organs ranged

from 0.73 to 4 µmol g^{-1} FW in shoots, and from 0.6 to 5.3 µmol g^{-1} FW in roots (Figures 1C and 1D).

Total P (*i.e.*, the sum of inorganic and organic P) concentration in P-limited shoots ranged from 3 to

30 µmol g^{-1} FW (Supplemental Figure 2A, Supplemental Table 2). Large variation in shoot

anthocyanin concentration reflected differences in P-limited shoot P status (Figure 1F). The

variation in Pi concentration of P-limited organs was largely due to higher Pi acquisition in P-

replete condition, with Pi concentrations ranging from 5.5 to 39.6 µmol g^{-1} FW in P-replete shoots,

and from 3.7 to 19.1 µmol g^{-1} FW in P-replete roots (Figures 1C and 1D, Supplemental Table 2).

Total P concentration in P-replete shoots ranged from 12 to 55 µmol g^{-1} FW (Supplemental Figure

2A). An inhibition of primary root growth, often described as a generalized response of *A. thaliana*

roots to Pi limitation (Gutiérrez-Alanís et al., 2018), was not universal across accessions. Similar to

findings by Chevalier and colleagues (2003), some accessions did not arrest their primary root

growth upon Pi withdrawal and 30 accessions even showed increased root growth (Figures 1A and

1E, Supplemental Tables 2 and 3). By contrast, a reduction in shoot biomass was always observed

across all accessions in the P-limited treatment (Figure 1B). Thus, shoot -P/+P biomass ratio was

positively correlated with Pi concentration in P-limited shoots (r = 0.29, *p* = 3.21E-4, Supplemental

Figure 2B). Accessions with the lowest shoot total P levels in P-limited conditions generally also

had the highest iron concentration in leaves (Supplemental Figure 2A, Supplemental Table 2).

Counter-intuitively, -P/+P root biomass ratio and Pi concentration in P-limited roots were negatively

correlated (r = -0.21, *p* = 2.52E-3). This is most likely due to dilution of the root Pi pool by lateral

root growth, resulting in lower root and higher shoot Pi concentration. Together, these data show

that P resources accumulated during seedling establishment are crucial to support RSA changes

6

150 during Pi limitation while iron accumulation in shoots restricts P-limited root growth. Albeit

151 significant, correlations were very low overall, again indicating strong variability between

152 accessions.

153   Overall, the considerable variation of quantified traits across accessions allowed for a highly

154 resolved genetic analysis of underlying determinants by GWAS.

155 **GWAS reveals candidate genes involved in a more efficient Pi starvation response**

156   To identify genes regulating individual PSR traits, we performed GWAS using SNP data from

157 the RegMap panel and the 1001 Genome Project (Materials and Methods; Alonso-Blanco et al.,

158 2016; Horton et al., 2012). Using the 1001 Genome SNP panel, we identified 154 significant SNPs

159 ($-\log_{10}(P) \geq 7$) that showed strong genetic association with Pi concentration in P-limited roots and

160 shoots, anthocyanin concentration in P-limited shoots, and effective primary root length under P-

161 replete conditions (Supplemental Figure 3, Supplemental Table 4). Using the RegMap panel SNPs,

162 we identified seven significant SNPs for two PSR traits ($-\log_{10}(P) > 6.4$), including one genomic

163 region associated with root biomass ratio (-P/+P). SNPs in the same genomic region were also

164 associated with root biomass ratio with the 1001 Genome SNP panel but fell just below the

165 selection threshold ($-\log_{10}(P)$ of 6.95 and 6.83, respectively; Supplemental Figure 3; Supplemental

166 Table 4). These significant SNPs resided in 70 candidate genes (Supplemental Figure 3;

167 Supplemental Table 4). To narrow down the candidate list, we cross-referenced the expression

168 profile of these candidate genes using published RNA-seq data (Linn et al., 2017, Supplemental

169 Table 5). A combination of SNP *P* value, SNP impact, trait-of-interest and RNA-seq expression

170 profile of associated genes was considered to select two loci for further analyses: Five SNPs with

171 significant association to Pi concentration in P-limited shoots were located on chromosome 5

172 (Figure 2A to 2C). This locus contains four *PHT1* genes (*PHT1;6, PHT1;1*, *PHT1;3*, and *PHT1;2*),

173 with the latter three genes in the 12 kb region surrounding the lead SNP. We will therefore refer to

174 this locus as the *PHOSPHATE TRANSPORTER1* (*PHT1*) locus. In agreement, reverse

175 transcription quantitative PCR (RT-qPCR) confirmed that all three genes were significantly induced

176 in P-limited Col-0 roots (2-fold induction of *PHT1;1*, 85-fold induction of *PHT1;2*, 354-fold induction

177 of *PHT1;3*; Figure 2D). Another locus on chromosome 5 was associated with Pi concentration in P-

7

178 limited roots, a trait that is of great interest due to its negative correlation with -P/+P root biomass

179 ratio and its wider implications for RSA (Supplemental Figure 2B). This locus contains two Pi

180 starvation responsive genes: one encodes a putative auxin efflux carrier family protein, PIN-

181 LIKES7 *(*PILS7*),* and the other one encodes the amino acid transporter protein AMINO ACID

182 VACUOLAR TRANSPORTER3 (AVT3) (Figure 2E to 2G). A third gene of unknown function,

183 *AT5G66000*, showed no transcriptional response to Pi withdrawal (Figure 2H, Supplemental Table

184 5). RT-qPCR confirmed that *PILS7* is suppressed and *AVT3* is induced in P-limited over P-replete

185 Col-0 roots (Figure 2H). We will refer to this locus as *PILS7* because nine out of 11 significant

186 SNPs are in the genomic sequence of *PILS7* (Supplemental Table 4). Considering the important

187 roles of both Pi and auxin transport for P status, organ growth and RSA (Bhosale et al., 2018;

188 Perez-Torres et al., 2008), we focused on *PHT1* and *PILS7* loci for further analysis of causal

189 mechanisms.

190 **Loss-of-function alleles of *PHT1;1*, *PHT1;2*, and *PILS7* in Col-0 affect plant growth and**

191 **organ Pi levels**

192 To characterize the impact of genes in the *PHT1* and *PILS7* loci on acclimation of the Col-

193 0 reference genotype to low Pi supply, T-DNA insertion mutants of the five PSR genes (*PHT1;1*,

194 *PHT1;2*, *PHT1;3*, *PILS7*, *AVT3*) were tested for their Pi starvation response (Supplemental Figure

195 4, Material and Methods). In agreement with a previous study (Shin et al., 2004), the *pht1;1* mutant

196 showed a significant reduction in shoot fresh weight compared to that of wildtype in both Pi

197 conditions (Figures 3A). Pi concentrations in P-replete *pht1;1* roots and shoots were significantly

198 reduced by 35 % and 70 % compared to wildtype, respectively, reaffirming the prominent role of

199 PHT1;1 in Pi uptake (Figures 3C and 3D). The *pht1;2* mutant had the opposite effect on growth as

200 its shoot biomass was significantly higher than that of wildtype under P-replete conditions, as was

201 root biomass under P-limiting conditions (Figures 3A and 3B). However, there was no significant

202 difference in organ Pi accumulation between *pht1;2* and wildtype (Figures 3C and 3D). Loss of

203 function in Pi transporters causes retarded plant growth (Nagarajan et al., 2011; Remy et al., 2012),

204 so enhanced organ biomass of the *pht1;2* mutant suggests that PHT1;2 may either be a Pi

205 exporter, expressed in cell types associated with Pi translocation or have functions beyond Pi

206 transport. The *pht1;3* mutant showed no trait difference compared to wildtype. Across accessions,

207 the *PHT1* locus was associated with Pi concentration in P-limited shoots (Figure 2), however, in

208 the Col-0 background, there was no significant difference in shoot Pi concentrations between P-

209 limited *pht1* mutants and the control. Knock-out of *PHT1;1* seemed to impact P status of P-replete

210 seedlings instead (Figures 3C and 3D). In line with the GWAS results, the *pils7-1* allele caused

211 higher Pi accumulation in P-limited roots (25 %, Figure 3D). Both P-replete *PILS7* loss-of-function

212 mutants showed significant reductions in root biomass (32 %) and root Pi concentration (20 %,

213 Figures 3B and 3D). The *avt3* mutant did not display any P status-dependent physiological

214 changes compared to wildtype. These data suggest that *PILS7* is associated with Pi concentration

215 in P-limited roots, and that impaired PILS7 activity leads to reduced Pi uptake and / or Pi

216 translocation from root to shoot.

217 **pht1;1 and pils7 mutant alleles are impaired in Pi acquisition**

218 To determine whether changes in organ Pi accumulation were a result of altered Pi uptake

219 by roots, we conducted a Pi depletion assay using *PHT1* and *PILS7* locus mutants and compared

220 those to the *pho2-2 / ubc24-1* (SAIL_47_E01) (Aung et al., 2006) and *phr1-2* (SALK_067629C)

221 mutants (Nilsson et al., 2007). Consistent with the earlier reports, the *pho2-2* mutant exhibited

222 significantly enhanced Pi uptake, while uptake tended to be lower in the *phr1-2* mutant compared

223 to wildtype (Figure 3E). Similar to results by Shin and colleagues (2004), Pi uptake capacity of P-

224 limited *pht1;1* was reduced to 70% of that of wildtype under P-limited conditions, but we did not

225 observe significant differences compared to wildtype in P-replete condition. The *pht1;2* and *pht1;3*

226 mutants behaved like wildtype (Figure 3E), as did the *avt3* mutant. Both *pils7* mutant alleles

227 showed impaired Pi uptake under P limitation, with P-limited *pils7-1* and *pils7-2* having only 71%

228 and 70% of the wildtype uptake capacity, respectively (Figure 3E). Similar Pi uptake capacity

229 between *pht1;1*, *pils7* mutants and wildtype under P-replete conditions clashes with the

230 observation of a lower Pi concentration in P-replete *pht1;1* and *pils7* roots (Figure 3D). This could

231 be other Pi transporters compensating for the *pht1;1* knockout in the short term (Pi depletion from

232 the media in Figure 3E was measured after 8 h), but not in the long term (accumulative effect in

9

233   Figure 3D was measured seven days after transfer). In P-replete *pils7* mutants this effect could

234   either be achieved by impairing PHT1;1 function, or by altering root-to-shoot Pi translocation.

235   **Large scale rearrangement of the *PHT1* locus corresponds with lower Pi concentration in P-**

236   **limited shoots of haplogroup 2 accessions**

237   Next, we assessed how the allelic variation in *PHT1;1*, *PHT1;2* or *PHT1;3* identified by

238   GWAS is causal of the variation in shoot Pi concentration across the 200 accessions under low Pi

239   supply. Using the RegMap panel's 250K SNP data, we performed a haplotype analysis on the

240   genomic region encompassing *PHT1;1, PHT1;3* and *PHT1;2* (Figure 4A). The two haplogroups

241   showed significant difference in the Pi concentrations in P-limited shoots, with Pi levels in

242   haplogroup 1 accessions higher than those in haplogroup 2 (p = 0.00632, Figure 4B, Supplemental

243   Table 6). SNP patterns of those accessions that were sequenced by the 1001 Genome Project

244   revealed many variants segregating among accessions from haplogroup 2 compared to those of

245   haplogroup 1 as well as the Col-0 reference allele (Figure 4A). For both the *PHT1;1* and *PHT1;2*

246   coding regions, one SNP shared by representative accessions of haplogroup 2 led to a

247   conservative amino acid change in each (Figure 4A). Strikingly, representative haplogroup 2

248   accessions featured deletions in promoters, exons and introns (grey bars in Figure 4A, dotted red

249   boxes in Supplemental Figures 4A and 4C). Consequences of these SNPs and deletions for the

250   amino acid composition of PHT1;1 and PHT1;2 proteins from haplogroup 2 accessions and their

251   predicted membrane topology are presented in Supplemental Figure 5: Exon 2 deletions in

252   haplogroup 2 alleles of *PHT1;1* and *PHT1;2* cause a loss of the second last extracellular loop at

253   the transporters' C-termini which will dramatically alter overall membrane topology. Given that the

254   C-terminus contains two phosphorylation sites (S514 and S520 of PHT1;1) that affect

255   PHOSPHATE TRANSPORTER TRAFFIC FACILITATOR (PHF1)-mediated PHT1 exit from the

256   endoplasmic reticulum (ER), as well as the predicted ER exit site itself (Bayle et al., 2011), these

257   deletions are expected to dramatically affect PHT1 activity and / or regulation. The *PHT1;1* allele is

258   likely to be further functionally compromised due to two deletions in transmembrane domain VII

259   and the preceding cytoplasmic loop (dotted grey boxes in Supplemental Figure 5B). In haplogroup

260   2 accessions, PHT1;2 would be the only remaining, fully functional Pi transporter of the *PHT1*

10

locus. Even more striking, the entire *PHT1;3* gene is missing from haplogroup 2 accessions (Figure 4A). Expression profiling of *PHT1;3* in roots of select haplogroup 1 and haplogroup 2 accessions across Pi treatments confirmed that the transcript could not be detected in the latter (Figure 5A). Alignment of whole genome sequencing reads for these accessions against the Col-0 *PHT1* locus confirmed the deletion of the *PHT1;3* gene in haplogroup 2 accessions (Figure 5B).

In conclusion, copy-number variation with loss of *PHT1;3* and major rearrangement of the remaining two *PHT1* genes in haplogroup 2 accessions dramatically reduces Pi acquisition resulting in lower shoot Pi concentration and higher sensitivity to Pi limitation. Differences in *PHT1* gene content and sequence variation may reflect adaptations of haplogroups to Pi availability in their habitats with haplogroup 2 most likely originating from a P-rich environment.

Allelic variation at the *PILS7* locus is associated with root Pi concentration in P-limited accessions

For the *PILS7* locus, the Pi concentration in P-limited roots of haplogroup 1 accessions was significantly lower than that of haplogroup 2 accessions (Figure 4D, Supplemental Table 6). Due to the negative correlation between Pi concentration in P-limited roots and root biomass ratio (Supplemental Figure 2B), haplogroup 1 accessions are likely to be more tolerant to Pi withdrawal than those of haplogroup 2. To identify causal sequence polymorphisms, we compared 1001 Genome Project derived *PILS7* locus SNP information for select accessions in two contrasting haplogroups: Across the genomic region haplogroup 2 accessions harbor 22 common SNPs that are absent from those of haplogroup 1 (Figure 4C). Of the SNPs in the *PILS7* coding region, eight reside in exons and seven in introns of the haplogroup 2 allele (Figure 4C). Of the eight exonic SNPs, only one leads to a non-synonymous change from alanine (Ala) to threonine (Thr). The other seven SNPs are silent mutations (Figure 4C). Sanger sequencing of genomic *PILS7* sequences PCR-amplified from representative haplogroup 1 accession HSm and haplogroup 2 accession Liarum confirmed these SNP locations (Supplemental Figure 6). It furthermore revealed extensive insertions and deletions within the promoter and the 1st intron of these two *PILS7* alleles (blue boxes in Supplemental Figure 6).

11

288   There is very little information available on functional domains within PILS proteins, but

289   transmembrane helices are highly conserved among PILS family members, and thus may have

290   central roles in auxin carrier function. The cytosolic loops display a lesser degree of conservation

291   and may have regulatory functions (Barbez et al., 2012). The non-synonymous amino acid change

292   is located in the longest cytosolic loop of PILS7 (Supplemental Figure 7). Substitution of the Ala

293   residue at position 197 with Thr in group 2 accessions may change the regulation of PILS7,

294   possibly through protein phosphorylation at Thr^{197}. This posttranslational modification could alter

295   PILS7 activity or turnover, subsequently affecting auxin sequestration in the endoplasmic reticulum

296   (ER) and nuclear auxin signaling (Beziat et al., 2017; Feraru et al., 2019). Changes in auxin

297   gradients would then impact lateral root and root hair formation, and either directly or indirectly

298   impact on Pi uptake and / or Pi translocation.

299   SNPs and indels in the promoter and 1st intron could alter the expression and / or splicing of

300   *PILS7*, resulting in altered PILS7 protein abundance. Promoter analysis using PlantPAN 3.0 (Chow

301   et al., 2019) identified a key transcription factor (TF) binding region (Supplemental Figure 6,

302   Supplemental Table 7) that was unique to the HSm (haplogroup 1) *PILS7* allele. It featured binding

303   sites for transcription factors of the APETALA2 (AP2) / ETHYLENE RESPONSE FACTOR (ERF)

304   and AUXIN RESPONSE FACTOR (ARF) families. AP2/ERF transcription factors have been

305   associated with auxin-sensitive abiotic stress signaling in roots promoting the transcription of ARF-

306   family AUXIN / INDOLE ACETIC ACID (Aux/IAA) repressors in response to desiccation and

307   osmotic stress (Shani et al., 2017). All of the ARF transcription factors predicted to bind to the HSm

308   *PILS7* promoter (ARF2, ARF4, ARF5, ARF6, ARF7, ARF8 and ARF11, Supplemental Table 7)

309   have been associated with auxin-controlled root hair as well as primary and lateral root

310   development (Choi et al., 2018; Dastidar et al., 2019; Santos Teixeira & Ten Tusscher, 2019; Yin

311   et al., 2020). While ARF5 and ARF11 stimulated root hair elongation, ARF2 and ARF4 acted as

312   repressors (Choi et al., 2018). ARF7 – together with ARF19 – targets the *PHR1* promoter which

313   features three auxin-response elements that confer auxin-stimulated lateral root formation and

314   increased Pi uptake in P-limited *A. thaliana* seedlings (Huang et al., 2018). These findings suggest

315   increased auxin-sensitive abiotic stress responsiveness of the HSm (haplogroup 1) but not the

316   Liarum (haplogroup 2) *PILS7* allele. We therefore measured *PILS7* expression in roots of select

317   haplogroup 1 and 2 accessions under P-replete and P-limiting conditions (Supplemental Figure 8).

318   While across accessions, expression was higher in P-replete and lower in P-limited roots, *PILS7*

319   transcripts were significantly less abundant in P-limited roots of haplogroup 2 accessions by about

320   2-fold. Thus, the additional TF binding site in the haplogroup 1 / HSm allele may help sustain

321   *PILS7* expression in P-limited roots. To test whether differential *PILS7* expression was associated

322   with expression changes in genes associated with Pi uptake or translocation, *PHT1;1*, *PHT1;4*,

323   *PHO1* and *MIR399D* transcript profiles were also determined (Supplemental Figure 8). The four

324   genes showed the typical expression profile reported for P-limited Col-0 roots, with strong induction

325   of *MIR399D* and *PHT1;4*, moderate induction of *PHT1;1* and no change in *PHO1* expression. None

326   of these genes showed differences in expression between haplogroups, indicating that observed

327   changes were *PILS7* specific.

328   Taken together, extensive allelic variation across the entire *PILS7* genomic sequence leads

329   to altered *PILS7* abundance and possibly altered post-translational regulation which would affect

330   root auxin signaling under stressful versus non-stressful conditions and cause the observed natural

331   variation in root Pi concentration and organ growth. It is unlikely that altered transcript expression

332   of PHO regulon components is responsible for trait variation.

333   **Elemental composition differs in the two contrasting haplogroups associated with *PHT1***

334   **and *PILS7* loci**

335   Shoot elemental composition data for each accession (Supplemental Figure 2A,

336   Supplemental Table 2) offered the opportunity to investigate the interaction of P with other

337   nutrients across the contrasting P-related haplogroups. Across accessions, the *PHT1* locus was

338   associated with variation of Pi concentration in P-limited shoots (Figure 4B). The elemental profiles

339   showed that total P (sum of inorganic and organic P) levels in P-limited shoots were similar

340   between haplogroups. However, P-replete haplogroup 1 accessions had higher leaf Pi and total P

341   concentration than haplogroup 2 accessions (Supplemental Figure 9A). This may suggest that due

342   to their three functional PHT1 paralogs, haplogroup 1 accessions are able to build up higher

343   organic P pools to boost growth under Pi limiting conditions.

344   For the *PILS7* locus, P-limited haplogroup 1 accessions had lower root Pi concentration

345   (Figure 4D). These accessions also have higher Pi concentration in P-replete organs and higher

346   root biomass irrespective of Pi supply (Supplemental Figure 9B). Total elemental composition

347   analysis revealed that their P-replete shoots also had higher total P levels (Supplemental Figure

348   9B), again suggesting higher mobilization capacity upon Pi withdrawal. Unlike *PHT1* locus

349   associated haplogroups, contrasting *PILS7* haplogroup accessions also differed in their leaf iron

350   and copper content. In P-limited environments, root architecture is also modified by iron and

351   copper availability (Perea-Garcia et al., 2013; Ward et al., 2008). Higher iron content in P-limited

352   leaves of haplogroup 2 accessions is consistent with lower shoot Pi and total P levels and confirms

353   their higher sensitivity to Pi withdrawal (Supplemental Figure 9B). Irrespective of P status, copper

354   concentration is always higher in leaves of haplogroup 2 accessions which can be an indicator of

355   altered PIN1-mediated auxin distribution (Yuan et al., 2013). High copper concentrations cause

356   primary root length inhibition via auxin depletion of the root apical meristem, a phenotype similar to

357   that seen here for *pils7* mutants (Figure 3B).

358   Despite similar nutrient allocation profiles, overlap in accessions between haplogroups 1 and

359   2 of *PHT1* and *PILS7* loci was low – with only three out of the 23 and 19 accessions shared in

360   haplogroup 1, and eight out of 30 and 29 accessions shared in haplogroup 2, respectively

361   (Supplemental Table 6). This would indicate that there has been no common selection for these

362   genetic marks.

363   **The *PILS7* allele of haplogroup 2 accessions fails to complement *PILS7* knockout in Col-0**

364   To further assess the impact of the contrasting Hsm and Liarum alleles on PILS7 function,

365   their genomic sequences were used for the complementation of the *pils7-1* mutant (Supplemental

366   Figure 10A). The *CaMV 35S* promoter-driven coding sequence of the Col-0 allele of *PILS7* was

367   also transformed into the *pils7-1* mutant background for comparison. The latter construct resulted

368   in strong (at least 435-fold) *PILS7* overexpression compared to Col-0 (Supplemental Figure 10B).

369   *35S::PILS7^Col-0* overexpression led to poor seedling and lateral root development as well as

370   stronger anthocyanin accumulation in shoots (Supplemental Figure 11E and 11F). Ectopic

371   expression of *PILS7* which – under its native promoter – is much more strongly expressed in Col-0

14

372   roots than shoots (Supplemental Figure 11G), thus appears to severely impair root auxin

373   distribution, perception or signaling, leading to growth impairment.

374   Across all progeny obtained for the two haplogroup alleles, the haplogroup 1 allele $PILS7^{HSm}$

375   led to distinctly higher expression than the haplogroup 2 allele $PILS7^{Liarum}$ (Supplemental Figures

376   10C and 10D). With each T1 line representing an independent T-DNA insertion, this could already

377   be an indication of differences in the relative promoter strengths of these two alleles. For each

378   allele, we chose two complementation lines for further characterization (high-lighted in

379   Supplemental Figures 10C and 10D). While *pils7-1* mutants expressing the haplogroup 1 allele

380     $PILS7^{HSm}$ to similar levels as the wild type allele in Col-0 were able to restore organ biomass and

381   Pi concentration of the *pils7-1* mutant back to Col-0 levels, the haplogroup 2 allele $PILS7^{Liarum}$ failed

382   to complement the *pils7-1* mutant when expressed at levels similar to the wild type allele or at

383   more than 150-fold higher levels (Figure 6; Supplemental Figure 10D). Despite strong

384   overexpression, the latter complementation line did also not lead to the retarded growth phenotype

385   observed in the $35S::PILS7^{Col-0}$ lines.

386   These results demonstrate that the two contrasting alleles not only have different promoter

387   strengths, but also result in functionally distinct PILS7 proteins. Genetic differences between them

388   are likely the result of adaptation to local P environments with haplogroup 1 *PILS7* alleles providing

389   improved auxin signaling in roots. This promotes more vigorous (lateral) root growth and higher Pi

390   uptake capacity enabling plants to actively seek out and exploit P-rich topsoil patches.

391   **Discussion**

392   *Complexity of genome-wide associations with key PSR traits*

393   In this study, we performed a GWAS on a number of traits associated with acclimation to low

394   Pi availability using *Arabidopsis thaliana* accessions of high genetic diversity (Li et al., 2010).

395   Unlike other studies that germinate seeds on media with contrasting Pi levels, our experimental

396   design aimed at identifying key determinants of more efficient Pi acquisition and utilization in the

397   presence of Pi, as seedlings were established on P-replete media prior to transfer to either low or

398   high Pi media. The selected traits showed variation across accessions, but only five traits showed

399   significant association with SNPs (Figure 2, Supplemental Figure 3, Supplemental Table 4). One

400   explanation for the limited number of associations with some traits might be that these are

401   controlled by a large number of genetic variants, each with only a modest contribution to the total

402   phenotypic variation. These minor-effect loci are only detectable when the size of study population

403   is big enough (Visscher et al., 2017). The fact that we found strong genetic determinants of root but

404   not shoot biomass ratio in P-limited over P-replete plants came as a surprise, given that root

405   growth relies on exported assimilate from shoots, and in non-stressed plants, a strong genetic

406   coupling between root and shoot growth has been found (Bouteillé et al., 2012). The requirement

407   to respond to environmental challenges would have made this relationship more complex over time.

408   The resulting complex genetic architecture of shoot growth can be a major challenge for GWAS

409   (Bouteillé et al., 2012; Marchadier et al., 2019). Nutrient limitation causes the strongest allocation

410   responses, with large increases in root biomass at the expense of stem and leaf biomass and no

411   significant difference between species from nutrient-poor and nutrient-rich habitats (Poorter et al.,

412   2012). The lack of variability in shoot biomass reduction across P-limited *A. thaliana* accessions

413   found in this study supports this hypothesis.

414   *Variation in copy number and protein topology of Pi transporters as potential sources of adaptation*

415   *to low phosphorus conditions*

416   Pi transporters of the PHT1 family are essential for Pi acquisition and Pi translocation,

417   however studies on their function have so far focused on the *A. thaliana* accession Col-0. Here, we

418   detected an association between the *PHT1* locus on chromosome 5 and Pi concentration in P-

419   limited shoots across 200 *A. thaliana* accessions. The locus identified on chromosome 5 contains

420   four *PHT1* paralog genes, most likely derived from a series of duplication events (Poirier & Bucher,

421   2002). From an evolutionary standpoint, gene duplication events in rate-limiting ion transporter

422   families, such as the PHT transporters, are sometimes associated with increased dosage, but

423   many are subjected to stronger purifying selection in the long term (Hudson et al., 2011). However,

424   so called 'fate determining mutations' can sub- or neofunctionalize duplicates and reduce selection

425   pressure whilst maintaining the original functional copy (Carretero-Paulet & Fares, 2012; Fournier-

426   Level et al., 2011; Innan & Kondrashov, 2010). Copy-number variants have been detected in

427   Arabidopsis accessions (Bush et al., 2014; Göktay et al., 2021; Jiao & Schneeberger, 2020; Long

16

428   et al., 2013; Zmienko et al., 2020). The most recent study of 1135 whole-genome sequenced

429   accessions from the 1001 Genomes Project identified copy-number variants associated with 18.5 %

430   of protein-coding regions, in particular regions of tandem duplications (Zmienko et al., 2020). Loss

431   of *PHT1;3* has been captured as CNV_18358. In haplogroup 2 accessions, the loss of *PHT1;3* and

432   substantial deletions in promoter and exon regions of *PHT1;1* and *PHT1;2* associated with

433   progressive loss of function could be an adaptation to environments with reliable Pi availability

434   (Figures 4A and 5, Supplemental Figure 5). Our finding that these accessions have lower Pi and

435   total P levels in P-limited shoots than those of haplogroup 1 confirms their reduced Pi uptake

436   capacity and higher sensitivity to Pi starvation (Supplemental Figure 9). In high P environments,

437   the *PHT1;3* gene might not be under the same selection pressure as in low P environments, and

438   its loss in haplogroup 2 accessions does not impact *in situ* performance (Supplemental Figure 9A).

439   The extra control loop that prevents hyperaccumulation of Pi in variable P environments by

440   phosphorylating the C-terminus of excess PHT1 proteins and retaining them in the ER (Bayle et al.,

441   2011) is not needed in habitats with more readily available Pi that incur only a moderate

442   expression of PHT1 protein in the first place (Supplemental Figure 5). In Col-0, PHT1;2 and

443   PHT1;3 are considered redundant (Ayadi et al., 2015) but only *PHT1;3* has been lost in haplogroup

444   2 accessions. We found that unlike other Pi transporter mutants in Col-0, *pht1;2* had higher organ

445   biomass than P-replete wildtype, and higher root biomass in P-limited conditions (Figure 3). Its

446   retention may therefore be due to its positive impact on plant growth. In wheat, the expression of Pi

447   transporters, and in particular *TaPHT1;2*, in response to Pi limitation differed between P-

448   acquisition-efficient and -inefficient cultivars, which also showed marked differences in organ- and

449   tissue-specific PSR traits (Aziz et al., 2014; de Souza Campos et al., 2019). In summary,

450   haplogroup 2 accessions carry genome modifications that are likely to reduce overall PHT1

451   transporter abundance at the plasma membrane as a reflection of adaptation to their local

452   environment.

453   *Hormonal signaling during PSR-induced changes in root system architecture*

454   Several phytohormones are involved in PSR, for example auxin, jasmonic acid and ethylene

455   (Bhosale et al., 2018; Borch et al., 1999; Khan et al., 2016; Perez-Torres et al., 2008;). Recent

17

studies show that auxin signaling is crucial for Pi starvation induced modifications of root system

architecture (Bhosale et al., 2018; Huang et al., 2018). The PIN-LIKES (PILS) family of auxin

transporters is comprised of seven members (PILS1 to PILS7) (Barbez et al., 2012). Individual

members of this family have recently been functionally characterized as ER-localized auxin carriers

that sequester auxin in the ER (Feraru et al., 2019), which in turn promotes auxin conjugation and

dampens nuclear auxin signaling. *PILS2* to *PILS7* transcript abundance increased with external

auxin application (Barbez et al., 2012). Overexpression of *PILS1* or *PILS3* led to shoot

developmental defects and dwarf plants. Knock-out of *PILS2* and *PILS5* promoted hypocotyl,

primary and lateral root growth (Barbez et al., 2012). This and other studies support a role of PILS

proteins as negative regulators of plant growth and development (Barbez et al., 2012; Beziat et al.,

2017; Feraru et al., 2019). By contrast, our results suggest that PILS7 is a positive regulator of

organ growth and Pi allocation as well as Pi acquisition by P-limited roots (Figure 3). Lack of

complementation of the *pils7-1* mutant by constitutive *PILS7* expression suggests a highly dose-

dependent, stress- and / or cell-specific role. Given its role in nuclear auxin depletion, PILS7

function could be associated with short-distance auxin transport and signaling during abiotic stress

(Korver et al., 2018). Its function could be to establish the cytokinin-dependent auxin minimum

needed to promote root cell differentiation and / or auxin oscillations required for lateral root

formation (De Rybel et al., 2010; Di Mambro et al., 2017). Similar to *pils7* mutants (Figure 6),

haplogroup 2 accessions have lower *PILS7* expression (Supplemental Figure 8) and higher Pi

concentration in P-limited roots (Figures 4D and Supplemental Figure 9B). The PILS7 protein of

haplogroup 2 is furthermore predicted to carry an extra phosphorylation site in its central

cytoplasmic loop (Supplemental Figure 7). These genomic modifications render the haplogroup 2

PILS7 allele incapable of rescuing the *pils7-1* mutant in the Col-0 background (Figure 6). The

negative correlation between P-limited root Pi concentration and root biomass ratio (-P/+P)

(Supplemental Figure 2B) would suggest that haplogroup 2 accessions come from P-rich habitats

and are more sensitive to Pi limitation. This is supported by their reduced capacity to take up Pi in

replete condition and the higher iron accumulation in P-limited shoots (Supplemental Figure 9B).

Selection pressure to sustain stress responsive *PILS7* promoter activity in these habitats may have

been low. The phosphorylation site in the haplogroup 2 PILS7 protein may be part of an additional

18

485   kinase/phosphatase signaling loop to help regulate auxin transporter activity in response to other

486   environmental or developmental clues. Haplogroup 1 accessions are more stress tolerant and

487   maintain higher organ Pi levels in P-replete conditions to support root growth upon Pi withdrawal

488   (Supplemental Figure 9B). The haplogroup 1 *PILS7* allele can complement the *pils7-1* mutant in

489   the Col-0 background (Figure 6). Unlike the Col-0 allele, its promoter is targeted by stress

490   responsive CBFs/ERFs and early ARF-dependent auxin signaling modules for lateral root

491   development (Santos Teixeira & Ten Tusscher, 2019) that help to sustain *PILS7* expression upon

492   Pi withdrawal (Supplemental Figure 8). The regulatory elements involved would suggest that – in

493   stress tolerant haplogroup 1 accessions - PILS7 is part of the TIR1- and ARF19-dependent

494   signaling cascade that stimulates the first asymmetric divisions in pericycle cells to promote lateral

495   root formation upon Pi withdrawal (Perez-Torres et al., 2008). How exactly PILS7 activity impacts

496   on nuclear auxin levels and ARF-dependent auxin and PSR signaling to promote root hair and

497   lateral root growth remains to be elucidated.

498   **Conclusion**

499   The results of this study revealed that higher Pi acquisition, Pi translocation from shoot to

500   root and higher investment in root biomass are critical for successful adaptation to a low Pi

501   environment. A switch in PHT1 isoform use, together with altered transcriptional and post-

502   translational regulation of PHT1 isoforms and PILS7 are tightly associated with these traits.

503   Interactions between these two loci are complex, however, with only a limited number of either

504   phosphate limitation tolerant or sensitive accessions sharing both genetic marks. The initial SNP

505   association led to the identification of more substantial genomic variation in alleles of individual

506   accessions that allowed us to identify additional aspects in the regulation of known players (PHT1

507   isoforms) and another player (PILS7) as key determinants of P efficiency that can inform plant

508   selection and improve fertilizer use in agronomic production systems.

Materials and Methods

Plant materials and growth conditions

509

510

511 The 200 Arabidopsis (*Arabidopsis thaliana*) accessions were kindly provided by Justin

512 Borevitz (Research School of Biology, The Australian National University, Canberra, Australia). In

513 order to identify differences in PSR without interference from seed quality, accessions were

514 propagated in the same temperature-controlled glasshouse and seeds were harvested from

515 individual plants showing the expected growth habit according to the germplasm details provided

516 by The Arabidopsis Information Resource (www.arabidopsis.org). Accessions requiring

517 vernalization (Supplemental Table 1) were transiently transferred to a temperature-controlled

518 cabinet for cold treatment. Names and identities of accessions as well as vernalization information

519 are provided in Supplemental Table 1.

520 T-DNA insertion lines were obtained from the Nottingham Arabidopsis Stock Centre (*pht1;2* /

521 SALK_110194C; *pht1;3* / GK-557C09; *pils7-1* / GK-768F05; *pils7-2* / SALK_069485; *avt3* /

522 SALK_010447C). Genotyping was carried out using primer combinations listed in Supplemental

523 Table 8A. T-DNA insertion sites in either the first or second exon of each mutant were confirmed

524 by Sanger sequencing (Supplemental Figure 4). Transcript abundance was determined via RT-

525 qPCR (Supplemental Figure 4). Previously published mutants, *pht1;1-2* (SALK_088586C, Shin et

526 al., 2004), *phr1-2* (SALK_067629C, Nilsson et al., 2007) and *pho2-2*/*ubc24-1* (SAIL_47_E01, Aung

527 et al., 2006) and Col-0 (N70000) were used as controls in the phenotyping experiments.

528 Plants for genotyping and propagation were grown in soil with 0.5 L coarse Vermiculite, 0.33

529 L Perlite, 33 g Nutricote^{TM} controlled-release fertilizer, 28 g ammonium nitrate, 25 g water-holding

530 granules, 15 g trace elements, and 7 g garden lime added per kg of standard potting mix (Van

531 Schaik's BioGro, Australia) under a 16-/8-hour light-dark cycle with 120 μmol m^{-2} s^{-1} light intensity,

532 at 22°C/19°C (light/dark), and 55 % relative humidity.

533 For the accession screen as well as phenotyping of T-DNA mutants and transgenic lines,

534 seeds were sterilized with chlorine gas for 2 hours, and then stratified at 4°C for 2 days in the dark.

535 Seedlings were germinated and grown on 10-cm square Petri dishes filled with 50 mL agar-

536 solidified Murashige & Skoog (MS) medium (Murashige & Skoog, 1962). After sowing of seeds, the

537 Petri dishes were placed in a near vertical position. The environmental settings were the same as

538 for soil-grown plants. The MS medium had the following composition: 0.61 g L^{-1} MS Modified Basal

539 Salt mixture (M407; Phytotech Laboratories), 20.6 mM NH_4NO_3, 18.8 mM KNO_3, 1 mM KH_2PO_4,

540 0.1% (w/v) MES, and 0.9% (w/v) Difco^{TM} Granulated Agar (LOT 6173985). For Pi depletion, 1 mM

541 KH_2PO_4 were replaced by 1 mM KCl. The solution was adjusted to pH 5.8 using 5 M KOH. The

542 residual Pi concentration of the agar used was 6.5 µM.

543   Accessions were established on MS medium, before seedlings with 2-cm-long primary roots

544 were transferred to either P-replete (1 mM Pi) or P-limited (6.5 µM Pi) medium and assessed after

545 seven days of growth (Supplemental Figure 1). Using seedlings of similar size across accessions

546 aimed at reducing the bias arising from maternal effects around seed quality and / or inherent

547 genetic differences in germination. Following an initial growth study, accessions were put into eight

548 groups defined by the number of days after sowing when the primary root length reached

549 approximate 2 cm (Supplemental Table 1). The seedlings were established for 4+x days in P-

550 replete medium, with x equaling the group number. To characterize T-DNA mutants in the Col-0

551 background, as well as *PILS7* overexpression and *pils7-1* complementation lines, seedlings were

552 established in P-replete medium until the primary root length reached approximate 2 cm, and then

553 transferred to either P-replete or P-limited medium and grown for another seven days prior to

554 harvesting root and shoot material.

555 **Tissue collection**

556   In the accession screen, one plate containing ten seedlings constituted one biological

557 replicate. Most accessions had three biological replicates per treatment and genotype, and a few

558 accessions only had two biological replicates due to poor germination (Supplemental Table 3). For

559 each plate, seedlings were separated into root and shoot for harvesting. Five individual shoots and

560 ten roots were combined into one sample for measuring Pi and anthocyanin (shoots only)

561 concentrations. For the characterization of transgenic lines, one plate containing eight seedlings

562 constituted one biological replicate. Each genotype had three biological replicates per treatment

563 and fresh weights were recorded for all samples, prior to shock-freezing in liquid N_2 and storing at -

564 80°C.

Primary root length measurement

Primary root length was determined as described earlier (Linn et al., 2017). Root images were analyzed in the ImageJ software using the SmartRoot plugin (Lobet et al., 2011). The effective primary root length was calculated by subtracting root length before transfer from root length at final harvest. The effective primary root lengths of P-replete or P-limited seedlings was used for GWAS.

Determination of Pi and anthocyanin concentration

To determine Pi and anthocyanin concentration, the frozen plant samples were ground and extracted with 1% (v/v) acetic acid at 4°C in the dark. Pi concentration was measured using the colorimetric ammonium molybdate assay as described earlier (Jost et al., 2015). Anthocyanin concentration in leaf samples was determined using a pH-differential method as described previously (Wrolstad et al., 2005).

Total P and elemental composition analysis

Accessions were grown as described (Supplemental Figure 1). Three shoot replicates were pooled to generate sufficient dry weight for acid digestion. The method for elemental analysis was adapted from Foroughi and colleagues (2014). Dry shoot material (ca. 10 mg) was digested with 300 μL of HCl : HNO_3 (3:1) at 70°C for 3 hours. Tomato (*Lycopersicon esculentum*) leaf reference material (Sigma Aldrich, NIST1573A) was used to validate the method accuracy. The digested samples were adjusted to a final volume of 10 mL of Milli-Q water and quantified by inductively coupled plasma mass spectrometry (ICP-MS).

Correlation analysis

The average of each measured trait was used for the correlation analysis, with two to three biological replicates for each accession (Supplemental Table 2). Correlation coefficients between the traits were calculated using the 'cor' function for Pearson's correlation in R (www.r-project.org). *p* values were calculated using 'cor_pmat' function in the ggcorrplot package (Version 0.1.3) in R.

22

Pi depletion assay

Seedlings were grown on P-replete MS medium for seven days and transferred to P-replete or P-limited medium for another seven days. Seedlings were then transferred to 2.5 mL of liquid P-replete MS medium in 24-well plates (Greiner CELLSTAR®, M9312), with five seedlings in each well. Aliquots of 200 μL MS medium were sampled prior to and eight hours after seedling addition. The Pi concentration of the medium was measured as described above to calculate the amount of Pi absorbed by the plants.

Statistical analysis of the measured traits

To account for possible batch effects, the best linear unbiased prediction (BLUP) of the phenotypic data was obtained, and the linear mixed effect function 'lmer' in the lme4 package of R (version 3.5.3) was used to fit the model (Borevitz et al., 2002). The model for the phenotypic trait was $Y_{ij} = u + Group_i + Genotype_j + e_{ij}$, where u is the total mean, $Group_i$ is the random group effect of the ith group, $Genotype_j$ is the random genetic effect of jth genotype, e_{ij} is a random error. The genotypic (breeding) value for each accession was computed as the Best Linear Unbiased Predictor (BLUP) of the genotype effect.

Genome wide association analysis

Out of the 200 accessions used in this study, 194 were covered by the RegMap panel and 104 by the 1001 Genome Project (Alonso-Blanco et al., 2016; Horton et al., 2012). BLUP values for each trait were used as phenotypic input for the GWAS analysis. GWAS was performed on the easyGWAS website (https://easygwas.ethz.ch) using the Efficient Mixed-Model Association eXpedited (EMMAX) algorithm that accounts for population structure (Grimm et al., 2016; Kang et al., 2010; Yu et al., 2006). SNPs with a minor allele frequency (MAF) of less than 0.05 were excluded from the analysis. The effective number of independent SNPs was calculated using a method described by Li and colleagues (2012). The effective number of independent SNPs for this study was calculated as 461,582 and 126,433 for the 1001 Genome Project and RegMap panel, respectively. A significance threshold of $α = 0.05$ was used after Bonferroni correction for multiple

23

testing. Manhattan plots were generated using the qqman package in R (version 3.5.3). The

location of genes closest to these significant SNPs were visualized by PhenoGram (Wolfe et al.,

2013).

Haplotype analysis

Haplotype analysis was performed as described previously (Li et al., 2014). Briefly, for the

194 accessions from the RegMap panel, SNPs located in the *PHT1* loci (from *PHT1;1* to *PHT1;3*)

and *PILS7* genes including a 3 kb promoter region were extracted (Horton et al., 2012). These

SNPs were used as the input for fastPHASE version 1.4.0 (Scheet & Stephens, 2006). The results

were analyzed and visualized in R (version 3.5.3).

Analysis of public sequencing data

Raw sequencing data of accessions (Ag-0, Wt-5, Do-0, Kelsterbach-4, and Sorbo) were

download from the NCBI Sequence Read Archive (Leinonen et al. & International Nucleotide

Sequence Database, 2011, https://www.ncbi.nlm.nih.gov/sra/?term=SRP056687). Sequencing

adapters and low-quality reads were trimmed with Trimmomatic (Version 0.32) (Bolger et al., 2014).

The trimmed reads were mapped to the *A. thaliana* reference accession Col-0 genome (TAIR

version 10) using HISAT2 (Version 2.1.0) and sorted using Samtools (Version 1.6) (Kim et al.,

2015; Li et al., 2009). The aligned sequences of Bay-0 (TAIR version 10) were downloaded from

the 1001 Genome project data center (Alonso-Blanco et al., 2016,

http://1001genomes.org/projects/JGIHeazlewood_2008/). Aligned sequences were

visualized using the Integrative Genomics Viewer (IGV) (Thorvaldsdottir et al., 2013).

Plasmid construction and plant transformation

To generate *35S::PILS7* overexpression lines, binary plasmids were constructed using

GATEWAY® cloning technology (ThermoFisher Scientific, Karimi et al., 2007). The coding

sequence without the *PILS7* stop codon was amplified from Col-0. Transgenic plants were selected

on MS medium containing 50 μg mL^{-1} kanamycin.

641   For complementation of the *pils7-1* mutant, the Gibson Assembly Cloning Kit (New England

642   Biolabs) was used for all constructs (Gibson et al., 2009). The *PILS7* gene, along with a 1928 bp

643   promoter fragment according to the Col-0 reference genome, was amplified from HSm and Liarum

644   genomic sequences. Primers used for cloning and sequencing of *PILS7* genomic sequences from

645   these two accessions are listed in Supplemental Table 8C. The amplified genomic fragments were

646   assembled into the binary vector pCAMBIA1300 (Hajdukiewicz et al., 1994) linearized with *EcoRI*

647   and *HindIII* (New England Biolabs). Transgenic plants were selected on 20 µg mL^{-1} hygromycin-

648   containing MS medium (Harrison et al., 2006).

649   All binary vector constructs were verified by sequencing (primers listed in Supplemental

650   Table 8C) and transformed into *Agrobacterium tumefaciens* strain GV3130. The floral dipping

651   technique was used to introduce all of the above constructs into the *pils7-1* mutant (Clough & Bent,

652   1998).

653   **Promoter analysis**

654   To identify binding motifs for *A. thaliana* transcription factors, promoter sequences of HSm

655   and Liarum *PILS7* alleles obtained from amplified genomic fragments (see cloning section above)

656   were used as input for the promoter analysis tool from PlantPAN 3.0 (Chow et al., 2019). Binding

657   motifs located on the sense strand of indels that discriminated between haplogroup alleles were

658   chosen for downstream analyses.

659   **RNA Isolation and Reverse Transcription Quantitative PCR**

660   Total RNA was isolated from root and shoot samples using the Spectrum Plant Total RNA kit

661   with on-column DNaseI digest according to the manufacturer (Sigma-Aldrich). The Tetro cDNA

662   Synthesis Kit (Bioline) was used for cDNA synthesis using 1 µg of total RNA as input. Quantitative

663   PCR was performed in a total reaction volume of 10 µL on the QuantStudio™ 12K Flex Real-Time

664   PCR system (Applied Biosystems). *UBIQUITIN CONJUGATING ENZYME9* (*UBC9*, AT4G27960)

665   and *UBC21* (AT5G25760) were used as reference genes. Relative expression level was calculated

666   using the 40-ΔCt method (Bari et al., 2006). Primers used for RT-qPCR are listed in Supplemental

667   Table 8B.

668 **Statistical analysis**

669   Statistical analyses were performed in R (version 3.5.3) using ANOVA, followed by Tukey's

670 pairwise multiple comparison of means. Unless stated otherwise, differences were considered

671 significant at $p < 0.05$, detailed statistical reports can be found in Supplemental Table 9.

672 **Accession Numbers**

673   Sequence data for the genes characterized in this article can be found in the Arabidopsis

674 Genome Initiative or GenBank / EMBL databases under the following accession numbers:

675 AT4G28610 (*PHOSPHATE STARVATION RESPONSE1*, *PHR1*), AT3G23430 (*PHOSPHATE1,*

676 *PHO1*), AT2G33770 (*PHOSPHATE2*, *PHO2*), AT2G34202 (*MICRORNA399D*, *MIR399D*),

677 AT5G43350 (*PHOSPHATE TRANSPORTER1;1*, *PHT1;1*), AT5G43370 (*PHOSPHATE*

678 *TRANSPORTER1;2*, *PHT1;2*), AT5G43360 (*PHOSPHATE TRANSPORTER1;3*, *PHT1;3*),

679 AT5G65980 (*PIN-LIKES 7*, *PILS7*), AT5G65990 (AMINO ACID VACUOLAR TRANSPORTER 3,

680 *AVT3*), AT5G66000 (unknown protein).

681 **Supplemental Data**

682 **Supplemental Figure S1: Experimental setup for accession screen.**

683

684 **Supplemental Figure S2: Shoot elemental composition and trait correlations in response to**

685 **Pi availability.**

686

687 **Supplemental Figure S3: Location of genes significantly associated with five key PSR traits.**

688 **Supplemental Figure S4: Characterization of T-DNA insertion mutants for '*PHT1*' and '*PILS7*'**

689 **loci genes in Col-0.**

690

691 **Supplemental Figure S5: Impact of indels on PHT1;1 and PHT1;2 protein sequences in**

692 **haplogroup 2 accessions.**

693

694 **Supplemental Figure S6: Genomic sequence variation in *PILS7* alleles from contrasting**

695 **haplotypes.**

696

697 **Supplemental Figure S7: Impact of the amino acid sequence variation in contrasting**

698 **haplogroups on PILS7 protein topology.**

699

700 **Supplemental Figure S8: Expression of *PILS7* and key PSR genes in ten accessions from**

701 **two distinct haplogroups.**

702

703 **Supplemental Figure S9: Natural variation in *PHT1* and *PILS7* loci corresponds to root fresh**

704 **weight, organ Pi, shoot total P, iron and copper concentrations.**

705

706 **Supplemental Figure S10: Generation and selection of *PILS7* overexpression and *pils7-1***

707 **complementation lines.**

708

709 **Supplemental Figure S11: Overexpression of *PILS7* in the *pils7-1* background does not**

710 **restore seedling growth and root Pi levels.**

711

712 **Supplemental Table S1**. Information on *A. thaliana* accessions screened in this study.

713 **Supplemental Table S2**. Summary of physiological and metabolic traits quantified in this study.

714 **Supplemental Table S3**. Raw data of fresh weight, primary root length, phosphate, and

715 anthocyanin concentrations.

716 **Supplemental Table S4**. List of GWAS candidate genes identified.

717 **Supplemental Table S5**. Expression profile of GWAS candidate genes in RNA-seq data set of P-

718 replete and P-limited Col-0 seedlings.

719 **Supplemental Table S6**. Haplotype analysis of genomic sequences of *PHT1* and *PILS7* loci.

720 **Supplemental Table S7**. *cis*-element analysis of *PILS7* promoters from HSm and Liarum

721 accessions.

722 **Supplemental Table S8**. List of primers used in this study.

723 **Supplemental Table S9**. Statistical reports for this study.

724 **Acknowledgments**

731 **Competing interests**

732 The authors declare no competing interests.

733 **Figure Legends**

734 **Figure 1. *A. thaliana* accessions vary significantly in their physiological and metabolic**

735 **response to Pi withdrawal.**

736 **A** and **B**, Violin plots of root (A) and shoot (B) biomass in P-replete and P-limited seedlings of 200

737 genetically diverse accessions. **C** and **D**, Violin plots of root (C) and shoot (D) Pi concentration in

738 P-replete and P-limited seedlings. **E**, Effective primary root length in P-replete and P-limiting

739 condition. **F**, Anthocyanin concentration in P-limited shoots. Anthocyanin concentrations in P-

740 replete shoots were below the assay's detection limit. **G**, Root and shoot biomass ratios (fresh

741 weight of P-limited versus P-replete organs). For reference, Col-0 data are highlighted in red. ND:

742 not determined. For each accession, the mean of two to three independent replicates was used

743 (Supplemental Table 2). The dot in the middle of the Violin plot indicates the mean of all

744 accessions and the vertical bar represents means ± SE. Statistical significance between treatments

745 was determined by one-way ANOVA. ** $p < 0.01$, *** $p < 0.001$.

746

Figure 2. Genome-wide association reveals loci responsible for variation in organ Pi levels in P-limited *A. thaliana* accessions.

A, Manhattan plots for association with Pi concentration in P-limited shoots. The dashed horizontal line indicates the Bonferroni-adjusted significance threshold ($-\log_{10}(p) = 7.0$). SNPs located within 5 kb of the lead SNP are labelled as red dots. **B**, Quantile–Quantile plot (Q-Q plot) for Pi concentration in P-limited shoots. **C**, Magnification of the genomic region surrounding the '*PHT1*' locus (12.3 kb). SNPs above the Bonferroni threshold are marked as red dots, gene models in this genomic region are shown below the x-axis. **D**, Transcript abundance of the candidate genes at the '*PHT1*' locus in P-replete (black bars) and P-limited (grey bars) roots of Col-0. **E** and **F**, Manhattan plot (E) and Q-Q plot (F) for genetic association with Pi concentration in P-limited roots, annotated as in panels **A** and **B**. **G**, Close-up of the genomic region surrounding the '*PILS7*' locus (12.3 kb). Annotations are the same as in panel **C**. **H**, Transcript levels of the candidate genes at the '*PILS7*' locus in P-replete and P-limited roots of Col-0. See panel **D** for detailed annotation. In **D** and **H**, each dot represents a biological replicate comprising eight seedlings grown vertically on a plate. Data are means ± SE. Statistical significance was determined by one-way ANOVA, ** $p < 0.01$, *** $p < 0.001$.

Figure 3: *pht1;1*, and *pils7* mutants show impaired growth, organ Pi accumulation and root Pi acquisition.

A and **B**, Fresh weight of shoots and roots of 14-day-old P-replete and P-limited seedlings. **C** and **D**, Phosphate concentration in shoots and roots of 14-day old seedlings. Experiments in panels **A** to **D** were performed in two separate batches, one for *PHT1* locus mutants and one for *PILS7* locus mutants. Each dot represents a biological replicate comprising eight seedlings grown vertically on a plate. Data are means ± SE. **E**, Pi acquisition by P-replete and P-limited roots. Results are from two independent experiments with three replicates of five seedlings each, with *pht1;1*, *pht1;3* and *avt3* only included in one experiment. Data are means ± SE. Asterisks indicate significant differences from Col-0 under each Pi treatment (One-way ANOVA and Tukey's HSD test, $p < 0.05$).

29

776 **Figure 4: Sequence variation in *PHT1* and *PILS7* loci is associated with natural variation in**

777 **organ Pi concentrations in P-limited seedlings.**

778 **A** and **C**, Genomic sequence surrounding the *PHT1* (A) and the *PILS7* locus (C) in five

779 representative accessions from the two most distinct haplogroups. Gene models (shown in green

780 at the top) represent those in Col-0. Colored vertical lines show single-bp substitutions with the

781 letter of the nucleotide shown next to the line; black vertical lines indicate single-bp deletions; grey

782 horizontal bars indicate larger deletions. Text and arrows below each panel indicate nucleotide and

783 amino acid substitutions shared by the five haplogroup 2 accessions; the non-conservative amino

784 acid change in PILS7 is labelled in red. SNPs shared uniquely by either haplogroup 1 or

785 haplogroup 2 accessions are indicated by # and vertical lines at the top and bottom of the

786 alignment, respectively. The large deletion within the *PHT1* locus encompassing *PHT1;3* is

787 highlighted by a red box. Pictures were generated from

788 http://signal.salk.edu/atg1001/3.0/gebrowser.php. **B** and **D**, Boxplots of normalized Pi

789 concentration in P-limited shoots (B) and roots (D) of accessions forming two distinct haplogroups

790 with respect to the *PHT1* (B) and *PILS7* locus (D). The lower and upper box edges correspond to

791 the first and third quartiles, the horizontal line indicates the median, the whiskers extend to

792 minimum and maximum values within 1.5✕ interquartile ranges. Statistical significance was

793 determined by one-way ANOVA ($p < 0.05$). LP: P-limited (6.5 µM). Hap1: Haplogroup 1; Hap2:

794 Haplogroup 2.

795

796 **Figure 5: The *PHT1;3* gene is absent from the genome of representative haplogroup 2**

797 **accessions.**

798 **A**, Pi-dependent *PHT1;3* expression in four representative accessions of the two most distinct

799 *PHT1* haplogroups. Each dot represents a biological replicate comprising ten seedlings grown

800 vertically on a plate. Data are means ± SE. In P-replete conditions, *PHT1;3* expression was

801 detected in two replicates of Ag-0, Bay-0, Wt-5, and only one replicate in Gu-0. Note that some of

802 the accessions chosen here differ from those shown in Figure 4A (For haplogroup 2, PHW-33 and

803 UKSE06-278 were not sequenced by 1001 Genome Project). **B**, Read coverage of sequenced

804 *PHT1* loci of three accessions from each of the two distinct haplotypes. Haplogroup 1 and 2

30

accessions are marked in blue and orange, respectively. ND: not detected. Hap1: Haplogroup 1;

Hap2: Haplogroup 2.

Figure 6: Natural allelic variation in *PILS7* impacts Pi-dependent growth and organ Pi allocation.

A and **B**, Shoot (A) and root (B) fresh weights of 14-day-old Col-0, *pils7-1* mutant and complementation lines carrying HSm or Liarum *PILS7* alleles. **C** and **D**, Organ Pi concentration of seedlings shown in **A** and **B**. HSm and Liarum are accessions from haplogroup 1 and haplogroup 2 accessions, respectively (Figure 4C). For *pils7-1* complementation, two individual lines for each haplotype allele were selected. Data are from two independent experiments with three biological replicates. Each dot represents a biological replicate comprising ten seedlings, the lower and upper box edges correspond to the first and third quartiles, the horizontal line indicates the median, the whiskers extend to minimum and maximum values within 1.5× interquartile ranges. Lines carrying the same *PILS7* allele were compared with Col-0 as one group. Asterisks indicate significant differences from Col-0 under each Pi-supply condition (One-way ANOVA and Tukey's HSD test, *, $p < 0.05$, **, $p < 0.01$, ***, $p < 0.001$).

822   **References**

823   Alonso-Blanco, C., Andrade, J., Becker, C., Bemm, F., Bergelson, J., Borgwardt, K. M., . . .

824   Genomes, C. (2016). 1,135 Genomes Reveal the Global Pattern of Polymorphism in

825   Arabidopsis thaliana. *Cell, 166*(2), 481-491. doi:10.1016/j.cell.2016.05.063

826   Aung, K., Lin, S. I., Wu, C. C., Huang, Y. T., Su, C. L., & Chiou, T. J. (2006). pho2, a phosphate

827   overaccumulator, is caused by a nonsense mutation in a microRNA399 target gene. *Plant*

828   *Physiology, 141*(3), 1000-1011. doi:10.1104/pp.106.078063

829   Ayadi, A., David, P., Arrighi, J.-F., Chiarenza, S., Thibaud, M.-C., Nussaume, L., & Marin, E. (2015).

830   Reducing the Genetic Redundancy of Arabidopsis PHOSPHATE TRANSPORTER1

831   Transporters to Study Phosphate Uptake and Signaling. *Plant Physiology, 167*(4), 1511-

832   1526. doi:10.1104/pp.114.252338

833   Aziz, T., Finnegan, P. M., Lambers, H., & Jost, R. (2014). Organ-specific phosphorus-allocation

834   patterns and transcript profiles linked to phosphorus efficiency in two contrasting wheat

835   genotypes. *Plant, Cell & Environment, 37*(4), 943-960. doi:10.1111/pce.12210

836   Barbez, E., Kubes, M., Rolcik, J., Beziat, C., Pencik, A., Wang, B. J., . . . Kleine-Vehn, J. (2012). A

837   novel putative auxin carrier family regulates intracellular auxin homeostasis in plants.

838   *Nature, 485*(7396), 119-U155. doi:10.1038/nature11001

839   Bari, R., Datt Pant, B., Stitt, M., & Scheible, W. R. (2006). PHO2, microRNA399, and PHR1 define

840   a phosphate-signaling pathway in plants. *Plant Physiology, 141*(3), 988-999.

841   doi:10.1104/pp.106.079707

842   Bates, T. R., & Lynch, J. P. (1996). Stimulation of root hair elongation in Arabidopsis thaliana by

843   low phosphorus availability. *Plant Cell and Environment, 19*(5), 529-538. doi:DOI

844   10.1111/j.1365-3040.1996.tb00386.x

845   Bayle, V., Arrighi, J.-F., Creff, A., Nespoulous, C., Vialaret, J., Rossignol, M., . . . Nussaume, L.

846   (2011). Arabidopsis thaliana high-affinity phosphate transporters exhibit multiple levels of

847   posttranslational regulation. *The Plant Cell, 23*(4), 1523-1535. doi: 10.1105/tpc.110.081067

848   Beziat, C., Barbez, E., Feraru, M. I., Lucyshyn, D., & Kleine-Vehn, J. (2017). Light triggers PILS-

849   dependent reduction in nuclear auxin signalling for growth transition. *Nat Plants, 3*, 17105.

850   doi:10.1038/nplants.2017.105

851   Bhosale, R., Giri, J., Pandey, B. K., Giehl, R. F. H., Hartmann, A., Traini, R., . . . Swarup, R. (2018).

852   A mechanistic framework for auxin dependent Arabidopsis root hair elongation to low

853   external phosphate. *Nature Communications, 9*(1), 1409. doi:10.1038/s41467-018-03851-3

854   Bolger, A.M., Lohse, M., & Usadel, B. (2014). Trimmomatic: A flexible trimmer for Illumina

855   sequence data. *Bioinformatics* 30(15): 2114–2120. doi: 10.1093/bioinformatics/

856   btu170.10.1093

857   Borch, K., Bouma, T. J., Lynch, J. P., & Brown, K. M. (1999). Ethylene: a regulator of root

858   architectural responses to soil phosphorus availability. *Plant Cell and Environment, 22*(4),

859   425-431. doi:DOI 10.1046/j.1365-3040.1999.00405.x

860   Borevitz, J. O., Maloof, J. N., Lutes, J., Dabi, T., Redfern, J. L., Trainer, G. T., . . . Chory, J. (2002).

861   Quantitative trait loci controlling light and hormone response in two accessions of

862   Arabidopsis thaliana. *Genetics, 160*(2), 683-696. doi: 10.1093/genetics/160.2.683

863   Bouain, N., Korte, A., Satbhai, S. B., Nam, H. I., Rhee, S. Y., Busch, W., & Rouached, H. (2019).

864   Systems genomics approaches provide new insights into Arabidopsis thaliana root growth

865   regulation under combinatorial mineral nutrient limitation. *Plos Genetics, 15*(11), e1008392.

866   doi:10.1371/journal.pgen.1008392

867   Bouteillé, M., Rolland, G., Balsera, C., Loudet, O., & Muller, B. (2012). Disentangling the

868   Intertwined Genetic Bases of Root and Shoot Growth in Arabidopsis. *Plos One, 7*(2),

869   e32319. doi:10.1371/journal.pone.0032319

870   Bush, S. J., Castillo-Morales, A., Tovar-Corona, J. M., Chen, L., Kover, P. X., & Urrutia, A. O.

871   (2014). Presence-absence variation in A. thaliana is primarily associated with genomic

872   signatures consistent with relaxed selective constraints. *Molecular Biology and Evolution,*

873   *31*(1), 59-69. doi:10.1093/molbev/mst166

874   Cakmak, I. (2002). Plant nutrition research: Priorities to meet human needs for food in sustainable

875   ways. *Plant and Soil, 247*(1), 3-24. doi:Doi 10.1023/A:1021194511492

33

876   Carretero-Paulet, L., & Fares, M. A. (2012). Evolutionary dynamics and functional specialization of

877   plant paralogs formed by whole and small-scale genome duplications. *Molecular Biology*

878   *and Evolution, 29*(11), 3541-3551. doi:10.1093/molbev/mss162

879   Ceasar, S. A., Baker, A., Muench, S. P., Ignacimuthu, S., & Baldwin, S. A. (2016). The

880   conservation of phosphate-binding residues among PHT1 transporters suggests that

881   distinct transport affinities are unlikely to result from differences in the phosphate-binding

882   site. *Biochemical Society Transactions, 44*(5), 1541-1548. doi:10.1042/BST20160016

883   Chevalier, F., Pata, M., Nacry, P., Doumas, P., & Rossignol, M. (2003). Effects of phosphate

884   availability on the root system architecture: large- scale analysis of the natural variation

885   between Arabidopsis accessions. *Plant, Cell & Environment, 26*(11), 1839-1850. doi:

886   10.1046/j.1365-3040.2003.01100.x

887   Choi, H. S., Seo, M., & Cho, H. T. (2018). Two TPL-Binding Motifs of ARF2 Are Involved in

888   Repression of Auxin Responses. *Front Plant Sci, 9*, 372. doi:10.3389/fpls.2018.00372

889   Chow, C. N., Lee, T. Y., Hung, Y. C., Li, G. Z., Tseng, K. C., Liu, Y. H., . . . Chang, W. C. (2019).

890   PlantPAN3.0: a new and updated resource for reconstructing transcriptional regulatory

891   networks from ChIP-seq experiments in plants. *Nucleic Acids Research, 47*(D1), D1155-

892   D1163. doi:10.1093/nar/gky1081

893   Clough, S. J., & Bent, A. F. (1998). Floral dip: a simplified method for Agrobacterium-mediated

894   transformation of Arabidopsis thaliana. *Plant Journal, 16*(6), 735-743. doi:10.1046/j.1365-

895   313x.1998.00343.x

896   Dastidar, M. G., Scarpa, A., Magele, I., Ruiz-Duarte, P., von Born, P., Bald, L., . . . Maizel, A.

897   (2019). ARF5/MONOPTEROS directly regulates miR390 expression in the Arabidopsis

898   thaliana primary root meristem. *Plant Direct, 3*(2), e00116. doi:10.1002/pld3.116

899   De Rybel, B., Vassileva, V., Parizot, B., Demeulenaere, M., Grunewald, W., Audenaert, D., . . .

900   Beeckman, T. (2010). A novel aux/IAA28 signaling cascade activates GATA23-dependent

901   specification of lateral root founder cell identity. *Current Biology, 20*(19), 1697-1706.

902   doi:10.1016/j.cub.2010.09.007

903   de Souza Campos, P. M., Cornejo, P., Rial, C., Borie, F., Varela, R. M., Seguel, A., & López-Ráez,

904   J. A. (2019). Phosphate acquisition efficiency in wheat is related to root:shoot ratio,

strigolactone levels, and PHO2 regulation. *Journal of Experimental Botany, 70*(20), 5631-5642. doi:10.1093/jxb/erz349

Di Mambro, R., De Ruvo, M., Pacifici, E., Salvi, E., Sozzani, R., Benfey, P. N., . . . Sabatini, S. (2017). Auxin minimum triggers the developmental switch from cell division to cell differentiation in the Arabidopsis root. *Proceedings of the National Academy of Sciences of the United States of America, 114*(36), E7641-E7649. doi:10.1073/pnas.1705833114

Feraru, E., Feraru, M. I., Barbez, E., Waidmann, S., Sun, L., Gaidora, A., & Kleine-Vehn, J. (2019). PILS6 is a temperature-sensitive regulator of nuclear auxin input and organ growth in Arabidopsis thaliana. *Proceedings of the National Academy of Sciences, 116*(9), 3893-3898. doi:10.1073/pnas.1814015116

Foroughi, S., Baker, A. J., Roessner, U., Johnson, A. A., Bacic, A., & Callahan, D. L. (2014). Hyperaccumulation of zinc by Noccaea caerulescens results in a cascade of stress responses and changes in the elemental profile. *Metallomics, 6*(9), 1671-1682. doi:10.1039/c4mt00132j

Fournier-Level, A., Hugueney, P., Verries, C., This, P., & Ageorges, A. (2011). Genetic mechanisms underlying the methylation level of anthocyanins in grape (Vitis vinifera L.). *BMC Plant Biology, 11*, 179. doi:10.1186/1471-2229-11-179

Gibson, D. G., Young, L., Chuang, R. Y., Venter, J. C., Hutchison, C. A., 3rd, & Smith, H. O. (2009). Enzymatic assembly of DNA molecules up to several hundred kilobases. *Nat Methods, 6*(5), 343-345. doi:10.1038/nmeth.1318

Göktay, M., Fulgione, A., & Hancock, A. M. (2020). A new catalogue of structural variants in 1301 A. thaliana lines from Africa, Eurasia and North America reveals a signature of balancing at defense response genes. Molecular Biology and Evolution. doi:10.1093/molbev/msaa309

Grimm, D. G., Roqueiro, D., Salome, P., Kleeberger, S., Greshake, B., Zhu, W., . . . Borgwardt, K. (2016). easyGWAS: A Cloud-based Platform for Comparing the Results of Genome-wide Association Studies. *The Plant Cell*. doi:10.1105/tpc.16.00551

Gutiérrez-Alanís, D., Ojeda-Rivera, J. O., Yong-Villalobos, L., Cárdenas-Torres, L., & Herrera-Estrella, L. (2018). Adaptation to Phosphate Scarcity: Tips from Arabidopsis Roots. *Trends in Plant Science, 23*(8), 721-730. doi:10.1016/j.tplants.2018.04.006

934 Hajdukiewicz P, Svab Z, Maliga P (1994). The small, versatile pPZP family of Agrobacterium

935   binary vectors for plant transformation. *Plant Molecular Biology, 25*(6), 989-94. doi:

936   10.1007/BF00014672.

937 Hamburger, D., Rezzonico, E., MacDonald-Comber Petetot, J., Somerville, C., & Poirier, Y. (2002).

938   Identification and characterization of the Arabidopsis PHO1 gene involved in phosphate

939   loading to the xylem. *The Plant Cell, 14*(4), 889-902. doi:10.1105/tpc.000745

940 Harrison, S. J., Mott, E. K., Parsley, K., Aspinall, S., Gray, J. C., & Cottage, A. (2006). A rapid and

941   robust method of identifying transformed Arabidopsis thaliana seedlings following floral dip

942   transformation. *Plant Methods, 2*(1), 19. doi:10.1186/1746-4811-2-19

943 Hinsinger, P. (2001). Bioavailability of soil inorganic P in the rhizosphere as affected by root-

944   induced chemical changes: a review. *Plant and Soil, 237*(2), 173-195. doi:Doi

945   10.1023/A:1013351617532

946 Horton, M. W., Hancock, A. M., Huang, Y. S., Toomajian, C., Atwell, S., Auton, A., . . . Bergelson, J.

947   (2012). Genome-wide patterns of genetic variation in worldwide Arabidopsis thaliana

948   accessions from the RegMap panel. *Nature Genetics, 44*(2), 212-216. doi:10.1038/ng.1042

949 Huang, K. L., Ma, G. J., Zhang, M. L., Xiong, H., Wu, H., Zhao, C. Z., . . . Ren, F. (2018). The

950   ARF7 and ARF19 Transcription Factors Positively Regulate PHOSPHATE STARVATION

951   RESPONSE1 in Arabidopsis Roots. *Plant Physiology, 178*(1), 413-427.

952   doi:10.1104/pp.17.01713

953 Hudson, C. M., Puckett, E. E., Bekaert, M., Pires, J. C., & Conant, G. C. (2011). Selection for

954   higher gene copy number after different types of plant gene duplications. *Genome Biol Evol,*

955   *3*, 1369-1380. doi:10.1093/gbe/evr115

956 Innan, H., & Kondrashov, F. (2010). The evolution of gene duplications: classifying and

957   distinguishing between models. *Nature Reviews Genetics, 11*(2), 97-108.

958   doi:10.1038/nrg2689

959 Jia, Z., Giehl, R. F. H., Meyer, R. C., Altmann, T., & von Wirén, N. (2019). Natural variation of

960   BSK3 tunes brassinosteroid signaling to regulate root foraging under low nitrogen. *Nature*

961   *Communications, 10*(1), 2378. doi:10.1038/s41467-019-10331-9

962 Jiao, W. B., & Schneeberger, K. (2020). Chromosome-level assemblies of multiple Arabidopsis

963   genomes reveal hotspots of rearrangements with altered evolutionary dynamics. *Nature*

964   *Communications, 11*(1), 989. doi:10.1038/s41467-020-14779-y

965 Jost, R., Pharmawati, M., Lapis-Gaza, H. R., Rossig, C., Berkowitz, O., Lambers, H., & Finnegan,

966   P. M. (2015). Differentiating phosphate-dependent and phosphate-independent systemic

967   phosphate-starvation response networks in Arabidopsis thaliana through the application of

968   phosphite. *Journal of Experimental Botany*. doi:10.1093/jxb/erv025

969 Kang, H. M., Sul, J. H., Service, S. K., Zaitlen, N. A., Kong, S.-y., Freimer, N. B., . . . Eskin, E.

970   (2010). Variance component model to account for sample structure in genome-wide

971   association studies. *Nature Genetics, 42*(4), 348-354. doi: 10.1038/ng.548

972 Karimi, M., Depicker, A., & Hilson, P. (2007). Recombinational cloning with plant gateway vectors.

973   *Plant Physiology, 145*(4), 1144-1154. doi:10.1104/pp.107.106989

974 Kawa, D., Julkowska, M. M., Sommerfeld, H. M., ter Horst, A., Haring, M. A., & Testerink, C. (2016).

975   Phosphate-Dependent Root System Architecture Responses to Salt Stress. *Plant*

976   *Physiology, 172*(2), 690-706. doi:10.1104/pp.16.00712

977 Khan, G. A., Vogiatzaki, E., Glauser, G., & Poirier, Y. (2016). Phosphate deficiency induces the

978   jasmonate pathway and enhances resistance to insect herbivory. *Plant Physiology*, pp.

979   00278.02016. doi: 10.1104/pp.16.00278

980 Kim, D., Langmead, B., & Salzberg, S. L. (2015). HISAT: a fast spliced aligner with low memory

981   requirements. *Nature Methods, 12*, 357. doi:10.1038/nmeth.3317

982 Kisko, M., Bouain, N., Safi, A., Medici, A., Akkers, R. C., Secco, D., . . . Rouached, H. (2018).

983   LPCAT1 controls phosphate homeostasis in a zinc-dependent manner. *eLife, 7*, e32077.

984   doi:10.7554/eLife.32077

985 Korver, R. A., Koevoets, I. T., & Testerink, C. (2018). Out of Shape During Stress: A Key Role for

986   Auxin. *Trends in Plant Science, 23*(9), 783-793. doi:10.1016/j.tplants.2018.05.011

987 Krysan, P. J., Young, J. C., & Sussman, M. R. (1999). T-DNA as an Insertional Mutagen in

988   Arabidopsis. *The Plant Cell, 11*(12), 2283-2290. doi:10.1105/tpc.11.12.2283

989   Leinonen, R., Sugawara, H., Shumway, M., & International Nucleotide Sequence Database, C.

990   (2011). The sequence read archive. *Nucleic Acids Research, 39*(Database issue), D19-21.

991   doi:10.1093/nar/gkq1019

992   Li, H., Handsaker, B., Wysoker, A., Fennell, T., Ruan, J., Homer, N., . . . Genome Project Data

993   Processing, S. (2009). The Sequence Alignment/Map format and SAMtools. *Bioinformatics,*

994   *25*(16), 2078-2079. doi:10.1093/bioinformatics/btp352

995   Li, M. X., Yeung, J. M., Cherny, S. S., & Sham, P. C. (2012). Evaluating the effective numbers of

996   independent tests and significant p-value thresholds in commercial genotyping arrays and

997   public imputation reference datasets. *Human Genetics, 131*(5), 747-756.

998   doi:10.1007/s00439-011-1118-2

999   Li, P., Filiault, D., Box, M. S., Kerdaffrec, E., van Oosterhout, C., Wilczek, A. M., . . . Nordborg, M.

1000   (2014). Multiple FLC haplotypes defined by independent cis-regulatory variation underpin

1001   life history diversity in Arabidopsis thaliana. *Genes & Development, 28*(15), 1635-1640. doi:

1002   10.1101/gad.245993.114

1003   Li, Y., Huang, Y., Bergelson, J., Nordborg, M., & Borevitz, J. O. (2010). Association mapping of

1004   local climate-sensitive quantitative trait loci in Arabidopsis thaliana. *Proceedings of the*

1005   *National Academy of Sciences of the United States of America, 107*(49), 21199-21204.

1006   doi:10.1073/pnas.1007431107

1007   Linn, J., Ren, M., Berkowitz, O., Ding, W., van der Merwe, M. J., Whelan, J., & Jost, R. (2017).

1008   Root Cell-Specific Regulators of Phosphate-Dependent Growth. *Plant Physiology, 174*(3),

1009   1969-1989. doi:10.1104/pp.16.01698

1010   Lobet, G., Pagès, L., & Draye, X. (2011). A novel image-analysis toolbox enabling quantitative

1011   analysis of root system architecture. *Plant Physiology, 157*(1), 29-39.

1012   Long, Q., Rabanal, F. A., Meng, D., Huber, C. D., Farlow, A., Platzer, A., . . . Nordborg, M. (2013).

1013   Massive genomic variation and strong selection in Arabidopsis thaliana lines from Sweden.

1014   *Nature Genetics, 45*(8), 884-890. doi:10.1038/ng.2678

1015   López-Arredondo, D. L., Leyva-González, M. A., González-Morales, S. I., López-Bucio, J., &

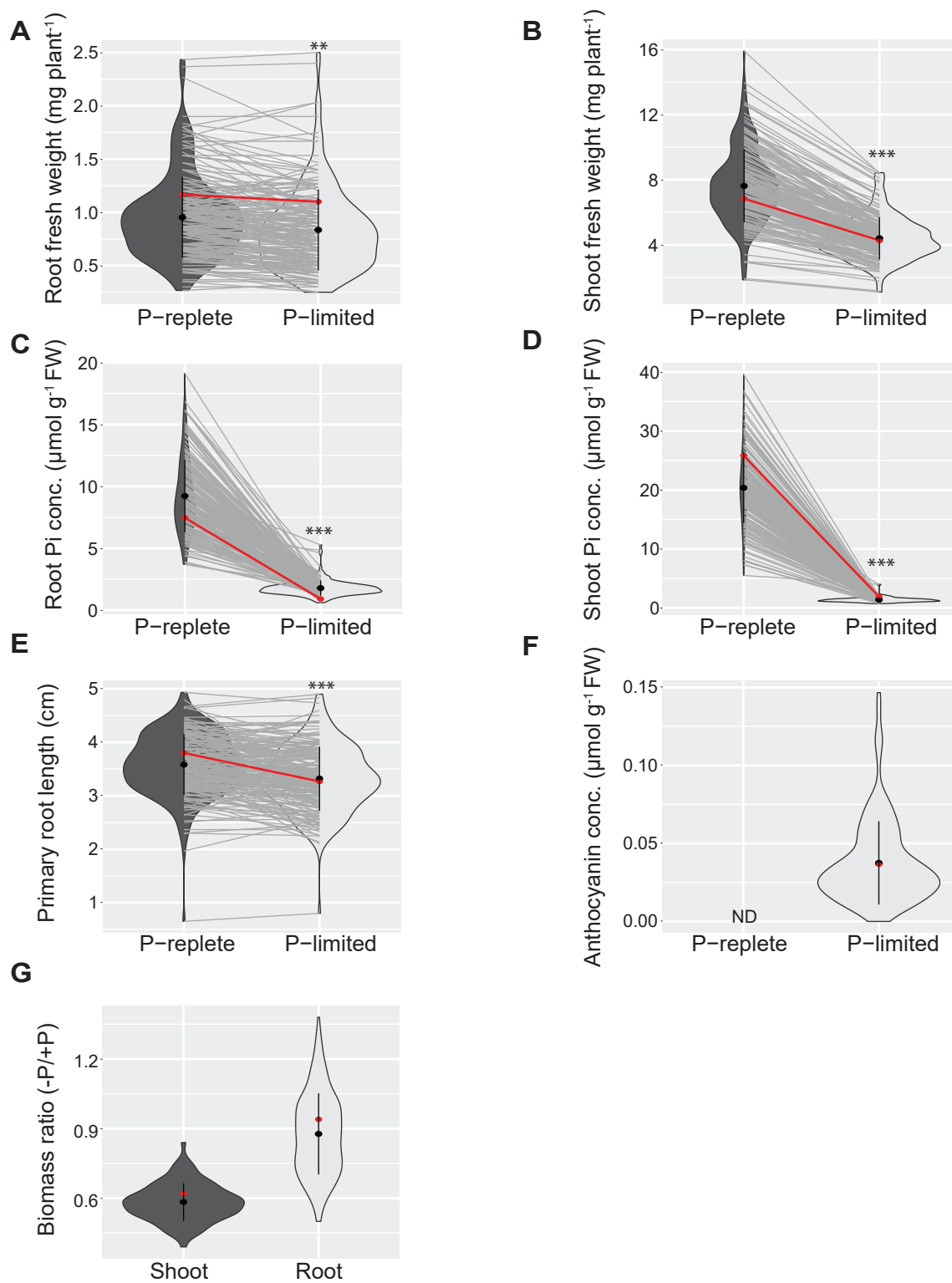1016   Herrera-Estrella, L. (2014). Phosphate Nutrition: Improving Low-Phosphate Tolerance in

1017   Crops. *Annual Review of Plant Biology, 65*(1), 95-123. doi:doi:10.1146/annurev-arplant-

1018   050213-035949

1019   López-Bucio, J., Hernández-Abreu, E., Sánchez-Calderón, L., Nieto-Jacobo, M. a. F., Simpson, J.,

1020   & Herrera-Estrella, L. (2002). Phosphate Availability Alters Architecture and Causes

1021   Changes in Hormone Sensitivity in the Arabidopsis Root System. *Plant Physiology, 129*(1),

1022   244-256. doi:10.1104/pp.010934

1023   Marchadier, E., Hanemian, M., Tisné, S., Bach, L., Bazakos, C., Gilbault, E., . . . Loudet, O. (2019).

1024   The complex genetic architecture of shoot growth natural variation in Arabidopsis thaliana.

1025   *Plos Genetics, 15*(4), e1007954. doi:10.1371/journal.pgen.1007954

1026   Mitchell, A. L., Attwood, T. K., Babbitt, P. C., Blum, M., Bork, P., Bridge, A., . . . Finn, R. D. (2019).

1027   InterPro in 2019: improving coverage, classification and access to protein sequence

1028   annotations. *Nucleic Acids Research, 47*(D1), D351-D360. doi:10.1093/nar/gky1100

1029   Muchhal, U. S., Pardo, J. M., & Raghothama, K. G. (1996). Phosphate transporters from the higher

1030   plant Arabidopsis thaliana. *Proceedings of the National Academy of Sciences of the United*

1031   *States of America, 93*(19), 10519-10523. doi:10.1073/pnas.93.19.10519

1032   Mudge, S. R., Rae, A. L., Diatloff, E., & Smith, F. W. (2002). Expression analysis suggests novel

1033   roles for members of the Pht1 family of phosphate transporters in Arabidopsis. *The Plant*

1034   *Journal, 31*(3), 341-353. doi: 10.1046/j.1365-313x.2002.01356.x

1035   Murashige, T., & Skoog, F. (1962). A Revised Medium for Rapid Growth and Bio Assays with

1036   Tobacco Tissue Cultures. *Physiologia Plantarum*, 15(3), 473-497. doi: 10.1111/j.1399-

1037   3054.1962.tb08052.x

1038   Nacry, P., Canivenc, G., Muller, B., Azmi, A., Van Onckelen, H., Rossignol, M., & Doumas, P.

1039   (2005). A Role for Auxin Redistribution in the Responses of the Root System Architecture

1040   to Phosphate Starvation in Arabidopsis. *Plant Physiology, 138*(4), 2061-2074.

1041   doi:10.1104/pp.105.060061

1042   Nagarajan, V. K., Jain, A., Poling, M. D., Lewis, A. J., Raghothama, K. G., & Smith, A. P. (2011).

1043   Arabidopsis Pht1; 5 mobilizes phosphate between source and sink organs and influences

1044   the interaction between phosphate homeostasis and ethylene signaling. *Plant Physiology,*

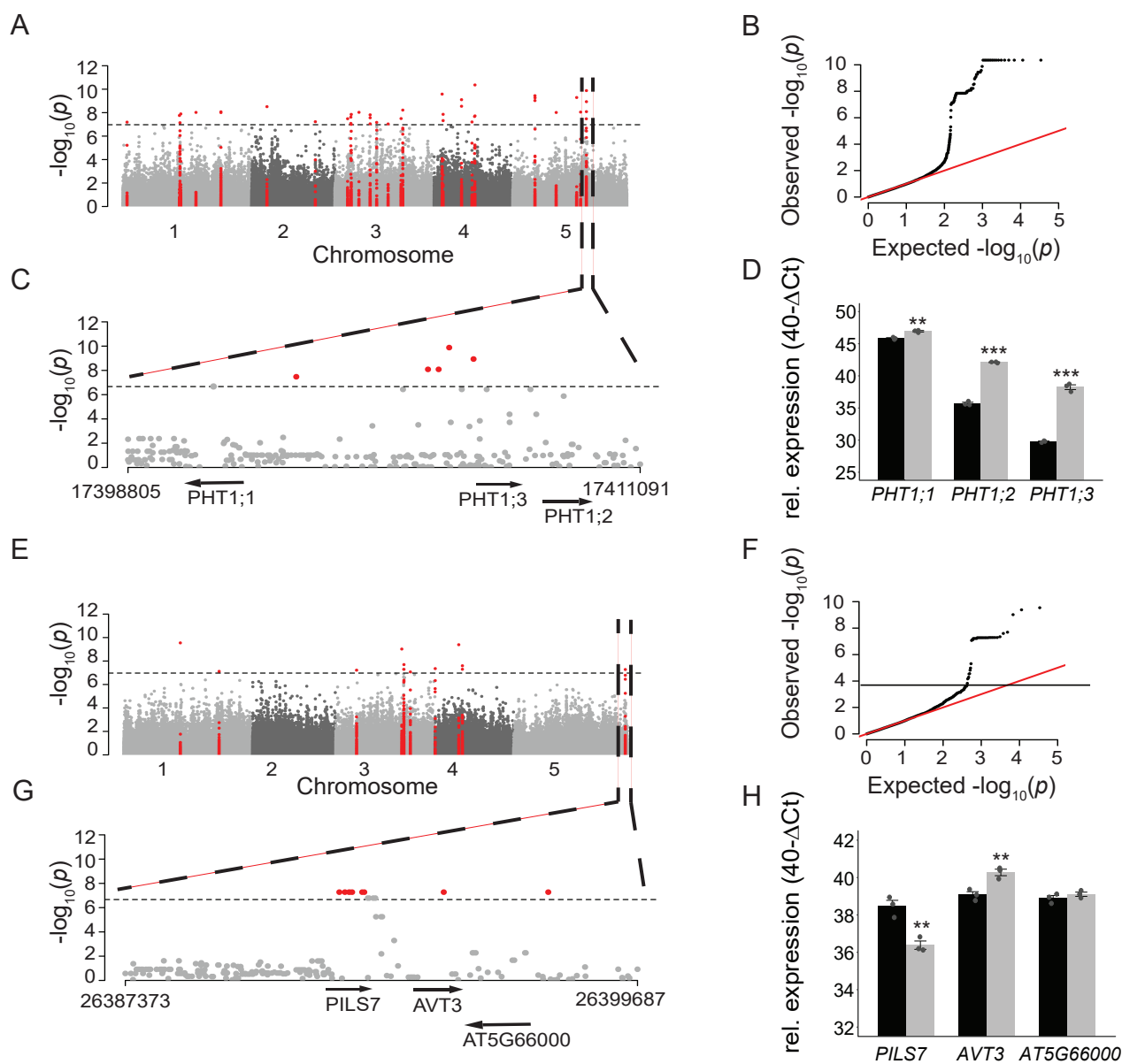1045   *156*(3), 1149-1163. doi: 10.1104/pp.111.174805

Nilsson, L., Müller, R., & Nielsen, T. H. (2007). Increased expression of the MYB- related

transcription factor, PHR1, leads to enhanced phosphate uptake in Arabidopsis thaliana.

Plant, Cell & Environment, 30(12), 1499-1512. doi: 10.1111/j.1365-3040.2007.01734.x

Perea-Garcia, A., Garcia-Molina, A., Andres-Colas, N., Vera-Sirera, F., Perez-Amador, M. A., Puig,

S., & Penarrubia, L. (2013). Arabidopsis copper transport protein COPT2 participates in the

cross talk between iron deficiency responses and low-phosphate signaling. *Plant*

Physiology, 162(1), 180-194. doi:10.1104/pp.112.212407

Perez-Torres, C. A., Lopez-Bucio, J., Cruz-Ramirez, A., Ibarra-Laclette, E., Dharmasiri, S., Estelle,

M., & Herrera-Estrella, L. (2008). Phosphate Availability Alters Lateral Root Development in

Arabidopsis by Modulating Auxin Sensitivity via a Mechanism Involving the TIR1 Auxin

Receptor. *The Plant Cell, 20*(12), 3258-3272. doi:10.1105/tpc.108.058719

Plaxton, W. C., & Tran, H. T. (2011). Metabolic Adaptations of Phosphate-Starved Plants. *Plant*

Physiology, 156(3), 1006-1015. doi:10.1104/pp.111.175281

Poirier, Y., & Bucher, M. (2002). Phosphate Transport and Homeostasis in Arabidopsis. *The*

Arabidopsis Book, 2002(1). doi:10.1199/tab.0024

Poorter, H., Niklas, K. J., Reich, P. B., Oleksyn, J., Poot, P., & Mommer, L. (2012). Biomass

allocation to leaves, stems and roots: meta-analyses of interspecific variation and

environmental control. *New Phytologist, 193*(1), 30-50. doi:10.1111/j.1469-

8137.2011.03952.x

Raghothama, K. (1999). Phosphate acquisition. *Annual Review of Plant Biology, 50*(1), 665-693.

doi: 10.1146/annurev.arplant.50.1.665

Remy, E., Cabrito, T., Batista, R., Teixeira, M., Sá- Correia, I., & Duque, P. (2012). The Pht1; 9

and Pht1; 8 transporters mediate inorganic phosphate acquisition by the Arabidopsis

thaliana root during phosphorus starvation. *New Phytologist, 195*(2), 356-371. doi:

10.1111/j.1469-8137.2012.04167.x

Rosas, U., Cibrian-Jaramillo, A., Ristova, D., Banta, J. A., Gifford, M. L., Fan, A. H., . . . Coruzzi, G.

M. (2013). Integration of responses within and across Arabidopsis natural accessions

uncovers loci controlling root systems architecture. *Proceedings of the National Academy of*

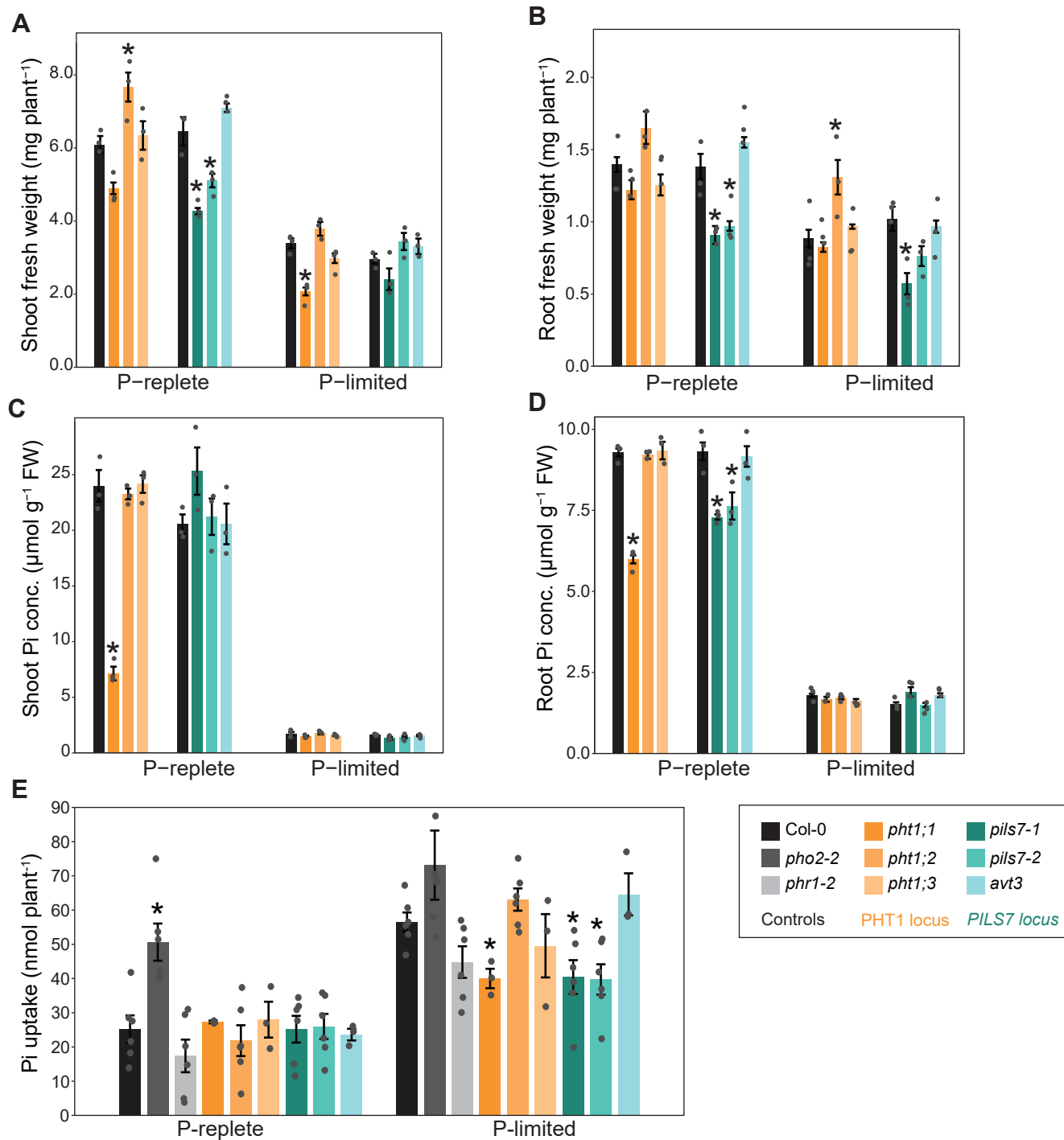1074   *Sciences of the United States of America, 110*(37), 15133-15138.

1075   doi:10.1073/pnas.1305883110

1076 Rubio, V., Linhares, F., Solano, R., Martin, A. C., Iglesias, J., Leyva, A., & Paz-Ares, J. (2001). A

1077   conserved MYB transcription factor involved in phosphate starvation signaling both in

1078   vascular plants and in unicellular algae. *Genes & Development, 15*(16), 2122-2133.

1079   doi:10.1101/gad.204401

1080 Sakuraba, Y., Kanno, S., Mabuchi, A., Monda, K., Iba, K., & Yanagisawa, S. (2018). A

1081   phytochrome-B-mediated regulatory mechanism of phosphorus acquisition. *Nat Plants,*

1082   *4*(12), 1089-1101. doi:10.1038/s41477-018-0294-7

1083 Santos Teixeira, J. A., & Ten Tusscher, K. H. (2019). The Systems Biology of Lateral Root

1084   Formation: Connecting the Dots. *Molecular Plant, 12*(6), 784-803.

1085   doi:10.1016/j.molp.2019.03.015

1086 Satbhai, S. B., Setzer, C., Freynschlag, F., Slovak, R., Kerdaffrec, E., & Busch, W. (2017). Natural

1087   allelic variation of FRO2 modulates Arabidopsis root growth under iron deficiency. *Nature*

1088   *Communications, 8*, 15603. doi:10.1038/ncomms15603

1089 Scheet, P., & Stephens, M. (2006). A fast and flexible statistical model for large-scale population

1090   genotype data: applications to inferring missing genotypes and haplotypic phase. *The*

1091   *American Journal of Human Genetics, 78*(4), 629-644. doi:10.1086/502802

1092 Shahzad, Z., & Amtmann, A. (2017). Food for thought: how nutrients regulate root system

1093   architecture. *Current Opinion in Plant Biology, 39*, 80-87. doi:10.1016/j.pbi.2017.06.008

1094 Shani, E., Salehin, M., Zhang, Y., Sanchez, S. E., Doherty, C., Wang, R., . . . Estelle, M. (2017).

1095   Plant Stress Tolerance Requires Auxin-Sensitive Aux/IAA Transcriptional Repressors.

1096   *Current Biology, 27*(3), 437-444. doi:10.1016/j.cub.2016.12.016

1097 Shin, H., Shin, H. S., Dewbre, G. R., & Harrison, M. J. (2004). Phosphate transport in Arabidopsis:

1098   Pht1; 1 and Pht1; 4 play a major role in phosphate acquisition from both low- and high-

1099   phosphate environments. *The Plant Journal, 39*(4), 629-642. doi: 10.1111/j.1365-
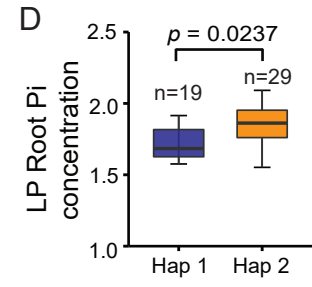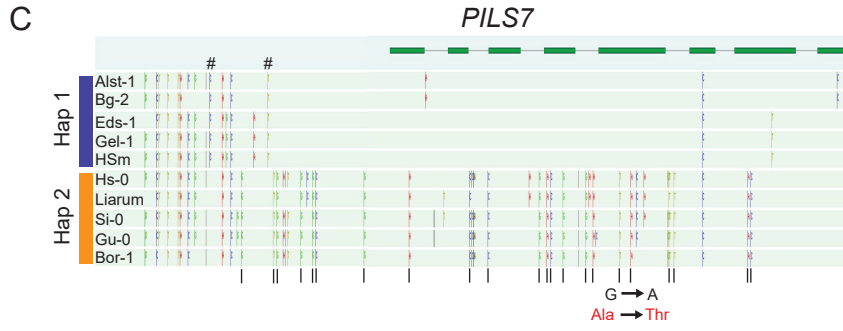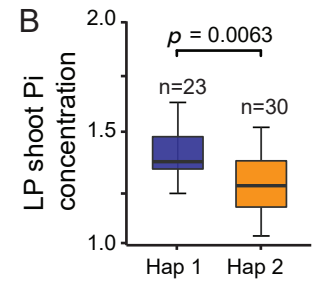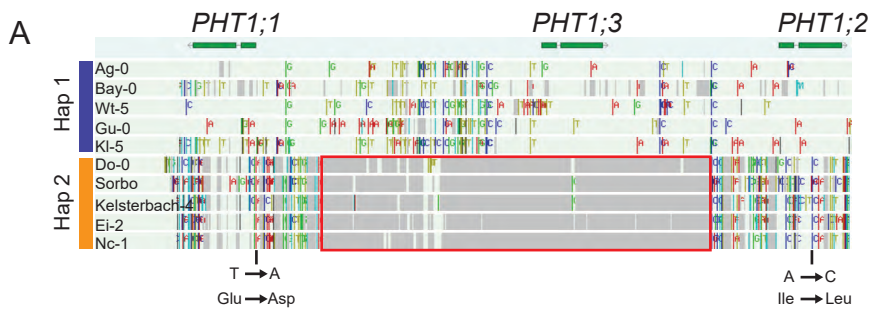
1100   313X.2004.02161.x

41

1101 Spyropoulos IC, Liakopoulos TD, Bagos PG, Hamodrakas SJ. (2004) TMRPres2D: high quality

1102   visual representation of transmembrane protein models. *Bioinformatics, 20*(17), 3258-60.

1103   doi: 10.1093/bioinformatics/bth358.

1104 The UniProt Consortium (2017). UniProt: the universal protein knowledgebase. *Nucleic Acids*

1105   *Research, 45*(D1), D158-D169. doi:10.1093/nar/gkw1099

1106 Thorvaldsdottir, H., Robinson, J. T., & Mesirov, J. P. (2013). Integrative Genomics Viewer (IGV):

1107   high-performance genomics data visualization and exploration. *Briefings in Bioinformatics,*

1108   *14*(2), 178-192. doi:10.1093/bib/bbs017

1109 Tusnady GE, Simon I. (2001) The HMMTOP transmembrane topology prediction server.

1110   *Bioinformatics, 17*(9), 849-50. doi: 10.1093/bioinformatics/17.9.849.

1111 Visscher, P. M., Wray, N. R., Zhang, Q., Sklar, P., McCarthy, M. I., Brown, M. A., & Yang, J. (2017).

1112   10 Years of GWAS Discovery: Biology, Function, and Translation. *The American Journal of*

1113   *Human Genetics, 101*(1), 5-22. doi:https://doi.org/10.1016/j.ajhg.2017.06.005

1114 Ward, J. T., Lahner, B., Yakubova, E., Salt, D. E., & Raghothama, K. G. (2008). The effect of iron

1115   on the primary root elongation of Arabidopsis during phosphate deficiency. *Plant*

1116   *Physiology, 147*(3), 1181-1191. doi:10.1104/pp.108.118562

1117 Wolfe, D., Dudek, S., Ritchie, M. D., & Pendergrass, S. A. (2013). Visualizing genomic information

1118   across chromosomes with PhenoGram. *BioData Min, 6*(1), 18. doi:10.1186/1756-0381-6-18

1119 Wrolstad, R. E., Durst, R. W., & Lee, J. (2005). Tracking color and pigment changes in anthocyanin

1120   products. *Trends in Food Science & Technology, 16*(9), 423-428.

1121 Yin, H., Li, M., Lv, M., Hepworth, S. R., Li, D., Ma, C., . . . Wang, S. M. (2020). SAUR15 Promotes

1122   Lateral and Adventitious Root Development via Activating H(+)-ATPases and Auxin

1123   Biosynthesis. *Plant Physiology, 184*(2), 837-851. doi:10.1104/pp.19.01250

1124 Yu, J., Pressoir, G., Briggs, W. H., Bi, I. V., Yamasaki, M., Doebley, J. F., . . . Holland, J. B. (2006).

1125   A unified mixed-model method for association mapping that accounts for multiple levels of

1126   relatedness. *Nature Genetics, 38*(2), 203-208. doi: 10.1038/ng1702

1127 Yuan, H. M., Xu, H. H., Liu, W. C., & Lu, Y. T. (2013). Copper regulates primary root elongation

1128   through PIN1-mediated auxin redistribution. *Plant and Cell Physiology, 54*(5), 766-778.

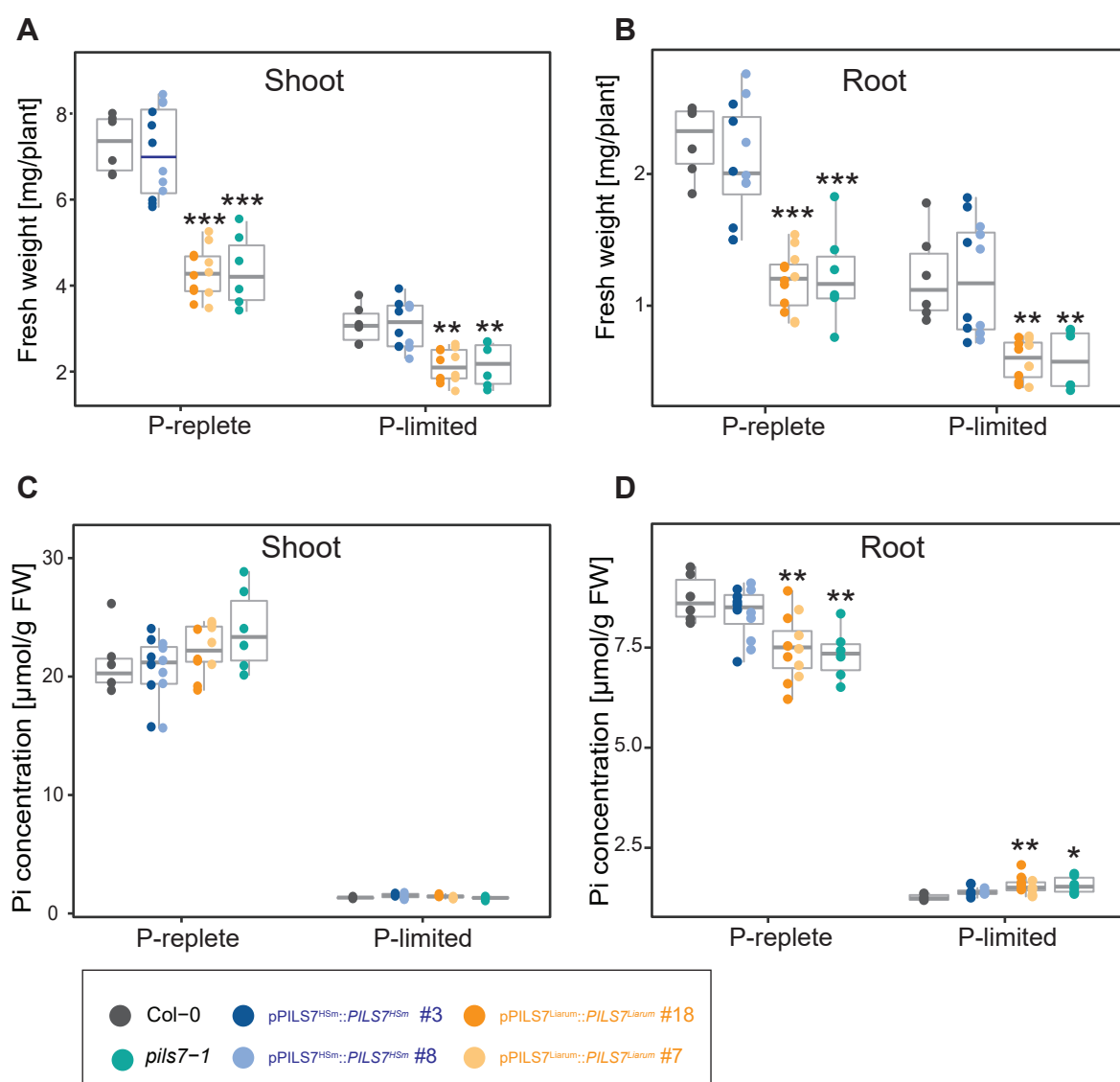1129   doi:10.1093/pcp/pct030

1130   Zmienko, A., Marszalek-Zenczak, M., Wojciechowski, P., Samelak-Czajka, A., Luczak, M.,

1131   Kozlowski, P., . . . Figlerowicz, M. (2020). AthCNV: A Map of DNA Copy Number Variations

1132   in the Arabidopsis Genome. *The Plant Cell, 32*(6), 1797-1819. doi:10.1105/tpc.19.00640
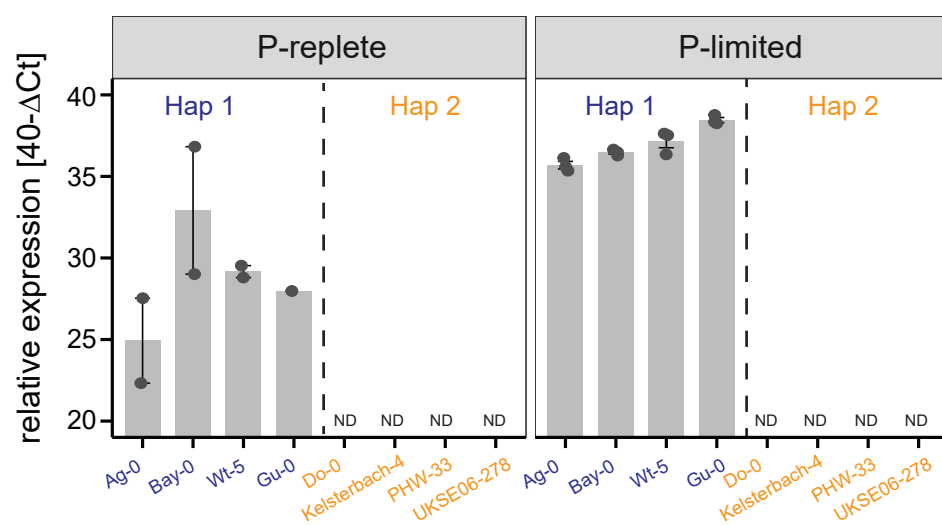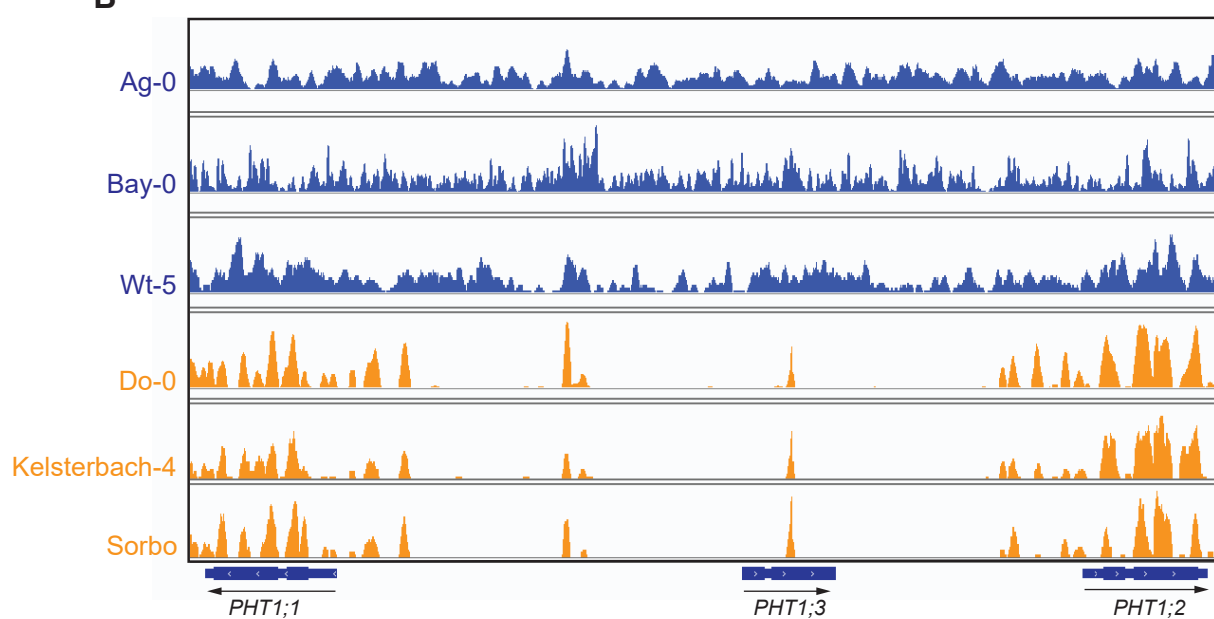
1133

A

Hap 1
- Ag-0
- Bay-0
- Wt-5
- Gu-0
- Kl-5

Hap 2
- Do-0
- Sorbo
- Kelsterbach-4
- Ei-2
- Nc-1

PHT1;1   *PHT1;3*   *PHT1;2*

T → A
Glu → Asp

A → C
Ile → Leu

B

$p = 0.0063$

n=23   n=30

LP shoot Pi concentration

Hap 1   Hap 2

C

PILS7

Hap 1
- Alst-1
- Bg-2
- Eds-1
- Gel-1
- HSm

Hap 2
- Hs-0
- Liarum
- Si-0
- Gu-0
- Bor-1

G → A
Ala → Thr

D

$p = 0.0237$

n=19   n=29

LP Root Pi concentration

Hap 1   Hap 2

A

P-replete | P-limited

Hap 1   Hap 2

relative expression [40-ΔCt]

Ag-0, Bay-0, Wt-5, Gu-0, Do-0, Kelsterbach-4, PHW-33, UKSE06-278

ND ND ND ND

B

Ag-0
Bay-0
Wt-5
Do-0
Kelsterbach-4
Sorbo

PHT1;1   *PHT1;3*   *PHT1;2*

Parsed Citations

Alonso-Blanco, C., Andrade, J., Becker, C., Bemm, F., Bergelson, J., Borgwardt, K. M., . . . Genomes, C. (2016). 1,135 Genomes Reveal the Global Pattern of Polymorphism in Arabidopsis thaliana. Cell, 166(2), 481-491. doi:10.1016/j.cell.2016.05.063
  Google Scholar: Author Only Title Only Author and Title

Aung, K., Lin, S. I., Wu, C. C., Huang, Y. T., Su, C. L., & Chiou, T. J. (2006). pho2, a phosphate overaccumulator, is caused by a nonsense mutation in a microRNA399 target gene. Plant Physiology, 141(3), 1000-1011. doi:10.1104/pp.106.078063
  Google Scholar: Author Only Title Only Author and Title

Ayadi, A., David, P., Arrighi, J.-F., Chiarenza, S., Thibaud, M.-C., Nussaume, L., & Marin, E. (2015). Reducing the Genetic Redundancy of Arabidopsis PHOSPHATE TRANSPORTER1 Transporters to Study Phosphate Uptake and Signaling. Plant Physiology, 167(4), 1511-1526. doi:10.1104/pp.114.252338
  Google Scholar: Author Only Title Only Author and Title

Aziz, T., Finnegan, P. M., Lambers, H., & Jost, R. (2014). Organ-specific phosphorus-allocation patterns and transcript profiles linked to phosphorus efficiency in two contrasting wheat genotypes. Plant, Cell & Environment, 37(4), 943-960. doi:10.1111/pce.12210
  Google Scholar: Author Only Title Only Author and Title

Barbez, E., Kubes, M., Rolcik, J., Beziat, C., Pencik, A, Wang, B. J., . . . Kleine-Vehn, J. (2012). A novel putative auxin carrier family regulates intracellular auxin homeostasis in plants. Nature, 485(7396), 119-U155. doi:10.1038/nature11001
  Google Scholar: Author Only Title Only Author and Title

Bari, R., Datt Pant, B., Stitt, M., & Scheible, W. R. (2006). PHO2, microRNA399, and PHR1 define a phosphate-signaling pathway in plants. Plant Physiology, 141(3), 988-999. doi:10.1104/pp.106.079707
  Google Scholar: Author Only Title Only Author and Title

Bates, T. R., & Lynch, J. P. (1996). Stimulation of root hair elongation in Arabidopsis thaliana by low phosphorus availability. Plant Cell and Environment, 19(5), 529-538. doi:DOI 10.1111/j.1365-3040.1996.tb00386.x
  Google Scholar: Author Only Title Only Author and Title

Bayle, V., Arrighi, J.-F., Creff, A, Nespoulous, C., Vialaret, J., Rossignol, M., . . . Nussaume, L. (2011). Arabidopsis thaliana high-affinity phosphate transporters exhibit multiple levels of posttranslational regulation. The Plant Cell, 23(4), 1523-1535. doi: 10.1105/tpc.110.081067
  Google Scholar: Author Only Title Only Author and Title

Beziat, C., Barbez, E., Feraru, M. I., Lucyshyn, D., & Kleine-Vehn, J. (2017). Light triggers PILS-dependent reduction in nuclear auxin signalling for growth transition. Nat Plants, 3, 17105. doi:10.1038/nplants.2017.105
  Google Scholar: Author Only Title Only Author and Title

Bhosale, R., Giri, J., Pandey, B. K., Giehl, R. F. H., Hartmann, A, Traini, R., . . . Swarup, R. (2018). A mechanistic framework for auxin dependent Arabidopsis root hair elongation to low external phosphate. Nature Communications, 9(1), 1409. doi:10.1038/s41467-018-03851-3
  Google Scholar: Author Only Title Only Author and Title

Bolger, A.M., Lohse, M., & Usadel, B. (2014). Trimmomatic: A flexible trimmer for Illumina sequence data. Bioinformatics 30(15): 2114–2120. doi: 10.1093/bioinformatics/ btu170.10.1093
  Google Scholar: Author Only Title Only Author and Title

Borch, K., Bouma, T. J., Lynch, J. P., & Brown, K. M. (1999). Ethylene: a regulator of root architectural responses to soil phosphorus availability. Plant Cell and Environment, 22(4), 425-431. doi:DOI 10.1046/j.1365-3040.1999.00405.x
  Google Scholar: Author Only Title Only Author and Title

Borevitz, J. O., Maloof, J. N., Lutes, J., Dabi, T., Redfern, J. L., Trainer, G. T., . . . Chory, J. (2002). Quantitative trait loci controlling light and hormone response in two accessions of Arabidopsis thaliana. Genetics, 160(2), 683-696. doi: 10.1093/genetics/160.2.683
  Google Scholar: Author Only Title Only Author and Title

Bouain, N., Korte, A, Satbhai, S. B., Nam, H. I., Rhee, S. Y., Busch, W., & Rouached, H. (2019). Systems genomics approaches provide new insights into Arabidopsis thaliana root growth regulation under combinatorial mineral nutrient limitation. Plos Genetics, 15(11), e1008392. doi:10.1371/journal.pgen.1008392
  Google Scholar: Author Only Title Only Author and Title

Bouteillé, M., Rolland, G., Balsera, C., Loudet, O., & Muller, B. (2012). Disentangling the Intertwined Genetic Bases of Root and Shoot Growth in Arabidopsis. Plos One, 7(2), e32319. doi:10.1371/journal.pone.0032319
  Google Scholar: Author Only Title Only Author and Title

Bush, S. J., Castillo-Morales, A, Tovar-Corona, J. M., Chen, L., Kover, P. X., & Urrutia, A. O. (2014). Presence-absence variation in A. thaliana is primarily associated with genomic signatures consistent with relaxed selective constraints. Molecular Biology and Evolution, 31(1), 59-69. doi:10.1093/molbev/mst166
  Google Scholar: Author Only Title Only Author and Title

Cakmak, I. (2002). Plant nutrition research: Priorities to meet human needs for food in sustainable ways. Plant and Soil, 247(1), 3-24.

doi:Doi 10.1023/A:1021194511492

Google Scholar: Author Only Title Only Author and Title

Carretero-Paulet, L., & Fares, M. A. (2012). Evolutionary dynamics and functional specialization of plant paralogs formed by whole and small-scale genome duplications. Molecular Biology and Evolution, 29(11), 3541-3551. doi:10.1093/molbev/mss162

Google Scholar: Author Only Title Only Author and Title

Ceasar, S. A., Baker, A., Muench, S. P., Ignacimuthu, S., & Baldwin, S. A. (2016). The conservation of phosphate-binding residues among PHT1 transporters suggests that distinct transport affinities are unlikely to result from differences in the phosphate-binding site. Biochemical Society Transactions, 44(5), 1541-1548. doi:10.1042/BST20160016

Google Scholar: Author Only Title Only Author and Title

Chevalier, F., Pata, M., Nacry, P., Doumas, P., & Rossignol, M. (2003). Effects of phosphate availability on the root system architecture: large-scale analysis of the natural variation between Arabidopsis accessions. Plant, Cell & Environment, 26(11), 1839-1850. doi: 10.1046/j.1365-3040.2003.01100.x

Google Scholar: Author Only Title Only Author and Title

Choi, H. S., Seo, M., & Cho, H. T. (2018). Two TPL-Binding Motifs of ARF2 Are Involved in Repression of Auxin Responses. Front Plant Sci, 9, 372. doi:10.3389/fpls.2018.00372

Google Scholar: Author Only Title Only Author and Title

Chow, C. N., Lee, T. Y., Hung, Y. C., Li, G. Z., Tseng, K. C., Liu, Y. H., . . . Chang, W. C. (2019). PlantPAN3.0: a new and updated resource for reconstructing transcriptional regulatory networks from ChIP-seq experiments in plants. Nucleic Acids Research, 47(D1), D1155-D1163. doi:10.1093/nar/gky1081

Google Scholar: Author Only Title Only Author and Title

Clough, S. J., & Bent, A. F. (1998). Floral dip: a simplified method for Agrobacterium-mediated transformation of Arabidopsis thaliana. Plant Journal, 16(6), 735-743. doi:10.1046/j.1365-313x.1998.00343.x

Google Scholar: Author Only Title Only Author and Title

Dastidar, M. G., Scarpa, A., Magele, I., Ruiz-Duarte, P., von Born, P., Bald, L., . . . Maizel, A. (2019). ARF5/MONOPTEROS directly regulates miR390 expression in the Arabidopsis thaliana primary root meristem. Plant Direct, 3(2), e00116. doi:10.1002/pld3.116

Google Scholar: Author Only Title Only Author and Title

De Rybel, B., Vassileva, V., Parizot, B., Demeulenaere, M., Grunewald, W., Audenaert, D., . . . Beeckman, T. (2010). A novel aux/IAA28 signaling cascade activates GATA23-dependent specification of lateral root founder cell identity. Current Biology, 20(19), 1697-1706. doi:10.1016/j.cub.2010.09.007

Google Scholar: Author Only Title Only Author and Title

de Souza Campos, P. M., Cornejo, P., Rial, C., Borie, F., Varela, R. M., Seguel, A., & López-Ráez, J. A. (2019). Phosphate acquisition efficiency in wheat is related to root:shoot ratio, strigolactone levels, and PHO2 regulation. Journal of Experimental Botany, 70(20), 5631-5642. doi:10.1093/jxb/erz349

Google Scholar: Author Only Title Only Author and Title

Di Mambro, R., De Ruvo, M., Pacifici, E., Salvi, E., Sozzani, R., Benfey, P. N., . . . Sabatini, S. (2017). Auxin minimum triggers the developmental switch from cell division to cell differentiation in the Arabidopsis root. Proceedings of the National Academy of Sciences of the United States of America, 114(36), E7641-E7649. doi:10.1073/pnas.1705833114

Google Scholar: Author Only Title Only Author and Title

Feraru, E., Feraru, M. I., Barbez, E., Waidmann, S., Sun, L., Gaidora, A., & Kleine-Vehn, J. (2019). PILS6 is a temperature-sensitive regulator of nuclear auxin input and organ growth in *Arabidopsis thaliana*. Proceedings of the National Academy of Sciences, 116(9), 3893-3898. doi:10.1073/pnas.1814015116

Google Scholar: Author Only Title Only Author and Title

Foroughi, S., Baker, A. J., Roessner, U., Johnson, A. A., Bacic, A., & Callahan, D. L. (2014). Hyperaccumulation of zinc by Noccaea caerulescens results in a cascade of stress responses and changes in the elemental profile. Metallomics, 6(9), 1671-1682. doi:10.1039/c4mt00132j

Google Scholar: Author Only Title Only Author and Title

Fournier-Level, A., Hugueney, P., Verries, C., This, P., & Ageorges, A. (2011). Genetic mechanisms underlying the methylation level of anthocyanins in grape (Vitis vinifera L.). BMC Plant Biology, 11, 179. doi:10.1186/1471-2229-11-179

Google Scholar: Author Only Title Only Author and Title

Gibson, D. G., Young, L., Chuang, R. Y., Venter, J. C., Hutchison, C. A., 3rd, & Smith, H. O. (2009). Enzymatic assembly of DNA molecules up to several hundred kilobases. Nat Methods, 6(5), 343-345. doi:10.1038/nmeth.1318

Google Scholar: Author Only Title Only Author and Title

Göktay, M., Fulgione, A., & Hancock, A. M. (2020). A new catalogue of structural variants in 1301 A. thaliana lines from Africa, Eurasia and North America reveals a signature of balancing at defense response genes. Molecular Biology and Evolution. doi:10.1093/molbev/msaa309

Google Scholar: Author Only Title Only Author and Title

Grimm, D. G., Roqueiro, D., Salome, P., Kleeberger, S., Greshake, B., Zhu, W., . . . Borgwardt, K. (2016). easyGWAS: A Cloud-based

Platform for Comparing the Results of Genome-wide Association Studies. The Plant Cell. doi:10.1105/tpc.16.00551
Google Scholar: Author Only Title Only Author and Title

Gutiérrez-Alanís, D., Ojeda-Rivera, J. O., Yong-Villalobos, L., Cárdenas-Torres, L., & Herrera-Estrella, L. (2018). Adaptation to Phosphate Scarcity: Tips from *Arabidopsis* Roots. Trends in Plant Science, 23(8), 721-730. doi:10.1016/j.tplants.2018.04.006
Google Scholar: Author Only Title Only Author and Title

Hajdukiewicz P, Svab Z, Maliga P (1994). The small, versatile pPZP family of Agrobacterium binary vectors for plant transformation. Plant Molecular Biology, 25(6), 989-94. doi: 10.1007/BF00014672.
Google Scholar: Author Only Title Only Author and Title

Hamburger, D., Rezzonico, E., MacDonald-Comber Petetot, J., Somerville, C., & Poirier, Y. (2002). Identification and characterization of the Arabidopsis PHO1 gene involved in phosphate loading to the xylem. The Plant Cell, 14(4), 889-902. doi:10.1105/tpc.000745
Google Scholar: Author Only Title Only Author and Title

Harrison, S. J., Mott, E. K., Parsley, K., Aspinall, S., Gray, J. C., & Cottage, A. (2006). A rapid and robust method of identifying transformed Arabidopsis thaliana seedlings following floral dip transformation. Plant Methods, 2(1), 19. doi:10.1186/1746-4811-2-19
Google Scholar: Author Only Title Only Author and Title

Hinsinger, P. (2001). Bioavailability of soil inorganic P in the rhizosphere as affected by root-induced chemical changes: a review. Plant and Soil, 237(2), 173-195. doi:Doi 10.1023/A:1013351617532
Google Scholar: Author Only Title Only Author and Title

Horton, M. W., Hancock, A. M., Huang, Y. S., Toomajian, C., Atwell, S., Auton, A., . . . Bergelson, J. (2012). Genome-wide patterns of genetic variation in worldwide Arabidopsis thaliana accessions from the RegMap panel. Nature Genetics, 44(2), 212-216. doi:10.1038/ng.1042
Google Scholar: Author Only Title Only Author and Title

Huang, K. L., Ma, G. J., Zhang, M. L., Xiong, H., Wu, H., Zhao, C. Z., . . . Ren, F. (2018). The ARF7 and ARF19 Transcription Factors Positively Regulate PHOSPHATE STARVATION RESPONSE1 in Arabidopsis Roots. Plant Physiology, 178(1), 413-427. doi:10.1104/pp.17.01713
Google Scholar: Author Only Title Only Author and Title

Hudson, C. M., Puckett, E. E., Bekaert, M., Pires, J. C., & Conant, G. C. (2011). Selection for higher gene copy number after different types of plant gene duplications. Genome Biol Evol, 3, 1369-1380. doi:10.1093/gbe/evr115
Google Scholar: Author Only Title Only Author and Title

Innan, H., & Kondrashov, F. (2010). The evolution of gene duplications: classifying and distinguishing between models. Nature Reviews Genetics, 11(2), 97-108. doi:10.1038/nrg2689
Google Scholar: Author Only Title Only Author and Title

Jia, Z, Giehl, R. F. H., Meyer, R. C., Altmann, T., & von Wirén, N. (2019). Natural variation of BSK3 tunes brassinosteroid signaling to regulate root foraging under low nitrogen. Nature Communications, 10(1), 2378. doi:10.1038/s41467-019-10331-9
Google Scholar: Author Only Title Only Author and Title

Jiao, W. B., & Schneeberger, K. (2020). Chromosome-level assemblies of multiple Arabidopsis genomes reveal hotspots of rearrangements with altered evolutionary dynamics. Nature Communications, 11(1), 989. doi:10.1038/s41467-020-14779-y
Google Scholar: Author Only Title Only Author and Title

Jost, R., Pharmawati, M., Lapis-Gaza, H. R., Rossig, C., Berkowitz, O., Lambers, H., & Finnegan, P. M. (2015). Differentiating phosphate-dependent and phosphate-independent systemic phosphate-starvation response networks in Arabidopsis thaliana through the application of phosphite. Journal of Experimental Botany. doi:10.1093/jxb/erv025
Google Scholar: Author Only Title Only Author and Title

Kang, H. M., Sul, J. H., Service, S. K., Zaitlen, N. A, Kong, S.-y., Freimer, N. B., . . . Eskin, E. (2010). Variance component model to account for sample structure in genome-wide association studies. Nature Genetics, 42(4), 348-354. doi: 10.1038/ng.548
Google Scholar: Author Only Title Only Author and Title

Karimi, M., Depicker, A., & Hilson, P. (2007). Recombinational cloning with plant gateway vectors. Plant Physiology, 145(4), 1144-1154. doi:10.1104/pp.107.106989
Google Scholar: Author Only Title Only Author and Title

Kawa, D., Julkowska, M. M., Sommerfeld, H. M., ter Horst, A, Haring, M. A., & Testerink, C. (2016). Phosphate-Dependent Root System Architecture Responses to Salt Stress. Plant Physiology, 172(2), 690-706. doi:10.1104/pp.16.00712
Google Scholar: Author Only Title Only Author and Title

Khan, G. A, Vogiatzaki, E., Glauser, G., & Poirier, Y. (2016). Phosphate deficiency induces the jasmonate pathway and enhances resistance to insect herbivory. Plant Physiology, pp. 00278.02016. doi: 10.1104/pp.16.00278
Google Scholar: Author Only Title Only Author and Title

Kim, D., Langmead, B., & Salzberg, S. L. (2015). HISAT: a fast spliced aligner with low memory requirements. Nature Methods, 12, 357. doi:10.1038/nmeth.3317
Google Scholar: Author Only Title Only Author and Title

Kisko, M., Bouain, N., Safi, A, Medici, A, Akkers, R. C., Secco, D., . . . Rouached, H. (2018). LPCAT1 controls phosphate homeostasis in a zinc-dependent manner. eLife, 7, e32077. doi:10.7554/eLife.32077
  Google Scholar: Author Only Title Only Author and Title

Korver, R. A, Koevoets, I. T., & Testerink, C. (2018). Out of Shape During Stress: A Key Role for Auxin. Trends in Plant Science, 23(9), 783-793. doi:10.1016/j.tplants.2018.05.011
  Google Scholar: Author Only Title Only Author and Title

Krysan, P. J., Young, J. C., & Sussman, M. R. (1999). T-DNA as an Insertional Mutagen in Arabidopsis. The Plant Cell, 11(12), 2283-2290. doi:10.1105/tpc.11.12.2283
  Google Scholar: Author Only Title Only Author and Title

Leinonen, R., Sugawara, H., Shumway, M., & International Nucleotide Sequence Database, C. (2011). The sequence read archive. Nucleic Acids Research, 39(Database issue), D19-21. doi:10.1093/nar/gkq1019
  Google Scholar: Author Only Title Only Author and Title

Li, H., Handsaker, B., Wysoker, A, Fennell, T., Ruan, J., Homer, N., . . . Genome Project Data Processing, S. (2009). The Sequence Alignment/Map format and SAMtools. Bioinformatics, 25(16), 2078-2079. doi:10.1093/bioinformatics/btp352
  Google Scholar: Author Only Title Only Author and Title

Li, M. X., Yeung, J. M., Cherny, S. S., & Sham, P. C. (2012). Evaluating the effective numbers of independent tests and significant p-value thresholds in commercial genotyping arrays and public imputation reference datasets. Human Genetics, 131(5), 747-756. doi:10.1007/s00439-011-1118-2
  Google Scholar: Author Only Title Only Author and Title

Li, P., Filiault, D., Box, M. S., Kerdaffrec, E., van Oosterhout, C., Wilczek, A. M., . . . Nordborg, M. (2014). Multiple FLC haplotypes defined by independent cis-regulatory variation underpin life history diversity in Arabidopsis thaliana. Genes & Development, 28(15), 1635-1640. doi: 10.1101/gad.245993.114
  Google Scholar: Author Only Title Only Author and Title

Li, Y., Huang, Y., Bergelson, J., Nordborg, M., & Borevitz, J. O. (2010). Association mapping of local climate-sensitive quantitative trait loci in Arabidopsis thaliana. Proceedings of the National Academy of Sciences of the United States of America, 107(49), 21199-21204. doi:10.1073/pnas.1007431107
  Google Scholar: Author Only Title Only Author and Title

Linn, J., Ren, M., Berkowitz, O., Ding, W., van der Merwe, M. J., Whelan, J., & Jost, R. (2017). Root Cell-Specific Regulators of Phosphate-Dependent Growth. Plant Physiology, 174(3), 1969-1989. doi:10.1104/pp.16.01698
  Google Scholar: Author Only Title Only Author and Title

Lobet, G., Pagès, L., & Draye, X. (2011). A novel image-analysis toolbox enabling quantitative analysis of root system architecture. Plant Physiology, 157(1), 29-39.
  Google Scholar: Author Only Title Only Author and Title

Long, Q., Rabanal, F. A, Meng, D., Huber, C. D., Farlow, A, Platzer, A, . . . Nordborg, M. (2013). Massive genomic variation and strong selection in Arabidopsis thaliana lines from Sweden. Nature Genetics, 45(8), 884-890. doi:10.1038/ng.2678
  Google Scholar: Author Only Title Only Author and Title

López-Arredondo, D. L., Leyva-González, M. A, González-Morales, S. I., López-Bucio, J., & Herrera-Estrella, L. (2014). Phosphate Nutrition: Improving Low-Phosphate Tolerance in Crops. Annual Review of Plant Biology, 65(1), 95-123. doi:doi:10.1146/annurev-arplant-050213-035949
  Google Scholar: Author Only Title Only Author and Title

López-Bucio, J., Hernández-Abreu, E., Sánchez-Calderón, L., Nieto-Jacobo, M. a. F., Simpson, J., & Herrera-Estrella, L. (2002). Phosphate Availability Alters Architecture and Causes Changes in Hormone Sensitivity in the Arabidopsis Root System. Plant Physiology, 129(1), 244-256. doi:10.1104/pp.010934
  Google Scholar: Author Only Title Only Author and Title

Marchadier, E., Hanemian, M., Tisné, S., Bach, L., Bazakos, C., Gilbault, E., . . . Loudet, O. (2019). The complex genetic architecture of shoot growth natural variation in Arabidopsis thaliana. Plos Genetics, 15(4), e1007954. doi:10.1371/journal.pgen.1007954
  Google Scholar: Author Only Title Only Author and Title

Mitchell, A. L., Attwood, T. K., Babbitt, P. C., Blum, M., Bork, P., Bridge, A, . . . Finn, R. D. (2019). InterPro in 2019: improving coverage, classification and access to protein sequence annotations. Nucleic Acids Research, 47(D1), D351-D360. doi:10.1093/nar/gky1100
  Google Scholar: Author Only Title Only Author and Title

Muchhal, U. S., Pardo, J. M., & Raghothama, K. G. (1996). Phosphate transporters from the higher plant Arabidopsis thaliana. Proceedings of the National Academy of Sciences of the United States of America, 93(19), 10519-10523. doi:10.1073/pnas.93.19.10519
  Google Scholar: Author Only Title Only Author and Title

Mudge, S. R., Rae, A. L., Diatloff, E., & Smith, F. W. (2002). Expression analysis suggests novel roles for members of the Pht1 family of phosphate transporters in Arabidopsis. The Plant Journal, 31(3), 341-353. doi: 10.1046/j.1365-313x.2002.01356.x
  Google Scholar: Author Only Title Only Author and Title

Murashige, T., & Skoog, F. (1962). A Revised Medium for Rapid Growth and Bio Assays with Tobacco Tissue Cultures. Physiologia Plantarum, 15(3), 473-497. doi: 10.1111/j.1399-3054.1962.tb08052.x

Google Scholar: Author Only Title Only Author and Title

Nacry, P., Canivenc, G., Muller, B., Azmi, A., Van Onckelen, H., Rossignol, M., & Doumas, P. (2005). A Role for Auxin Redistribution in the Responses of the Root System Architecture to Phosphate Starvation in Arabidopsis. Plant Physiology, 138(4), 2061-2074. doi:10.1104/pp.105.060061

Google Scholar: Author Only Title Only Author and Title

Nagarajan, V. K., Jain, A., Poling, M. D., Lewis, A. J., Raghothama, K. G., & Smith, A. P. (2011). Arabidopsis Pht1; 5 mobilizes phosphate between source and sink organs and influences the interaction between phosphate homeostasis and ethylene signaling. Plant Physiology, 156(3), 1149-1163. doi: 10.1104/pp.111.174805

Google Scholar: Author Only Title Only Author and Title

Nilsson, L., Müller, R., & Nielsen, T. H. (2007). Increased expression of the MYB-related transcription factor, PHR1, leads to enhanced phosphate uptake in Arabidopsis thaliana. Plant, Cell & Environment, 30(12), 1499-1512. doi: 10.1111/j.1365-3040.2007.01734.x

Google Scholar: Author Only Title Only Author and Title

Perea-Garcia, A, Garcia-Molina, A, Andres-Colas, N., Vera-Sirera, F., Perez-Amador, M. A, Puig, S., & Penarrubia, L. (2013). Arabidopsis copper transport protein COPT2 participates in the cross talk between iron deficiency responses and low-phosphate signaling. Plant Physiology, 162(1), 180-194. doi:10.1104/pp.112.212407

Google Scholar: Author Only Title Only Author and Title

Perez-Torres, C. A, Lopez-Bucio, J., Cruz-Ramirez, A, Ibarra-Laclette, E., Dharmasiri, S., Estelle, M., & Herrera-Estrella, L. (2008). Phosphate Availability Alters Lateral Root Development in Arabidopsis by Modulating Auxin Sensitivity via a Mechanism Involving the TIR1 Auxin Receptor. The Plant Cell, 20(12), 3258-3272. doi:10.1105/tpc.108.058719

Google Scholar: Author Only Title Only Author and Title

Plaxton, W. C., & Tran, H. T. (2011). Metabolic Adaptations of Phosphate-Starved Plants. Plant Physiology, 156(3), 1006-1015. doi:10.1104/pp.111.175281

Google Scholar: Author Only Title Only Author and Title

Poirier, Y., & Bucher, M. (2002). Phosphate Transport and Homeostasis in Arabidopsis. The Arabidopsis Book, 2002(1). doi:10.1199/tab.0024

Google Scholar: Author Only Title Only Author and Title

Poorter, H., Niklas, K. J., Reich, P. B., Oleksyn, J., Poot, P., & Mommer, L. (2012). Biomass allocation to leaves, stems and roots: meta-analyses of interspecific variation and environmental control. New Phytologist, 193(1), 30-50. doi:10.1111/j.1469-8137.2011.03952.x

Google Scholar: Author Only Title Only Author and Title

Raghothama, K. (1999). Phosphate acquisition. Annual Review of Plant Biology, 50(1), 665-693. doi: 10.1146/annurev.arplant.50.1.665

Google Scholar: Author Only Title Only Author and Title

Remy, E., Cabrito, T., Batista, R., Teixeira, M., Sá-Correia, I., & Duque, P. (2012). The Pht1; 9 and Pht1; 8 transporters mediate inorganic phosphate acquisition by the Arabidopsis thaliana root during phosphorus starvation. New Phytologist, 195(2), 356-371. doi: 10.1111/j.1469-8137.2012.04167.x

Google Scholar: Author Only Title Only Author and Title

Rosas, U., Cibrian-Jaramillo, A, Ristova, D., Banta, J. A, Gifford, M. L., Fan, A. H., . . . Coruzzi, G. M. (2013). Integration of responses within and across Arabidopsis natural accessions uncovers loci controlling root systems architecture. Proceedings of the National Academy of Sciences of the United States of America, 110(37), 15133-15138. doi:10.1073/pnas.1305883110

Google Scholar: Author Only Title Only Author and Title

Rubio, V., Linhares, F., Solano, R., Martin, A. C., Iglesias, J., Leyva, A, & Paz-Ares, J. (2001). A conserved MYB transcription factor involved in phosphate starvation signaling both in vascular plants and in unicellular algae. Genes & Development, 15(16), 2122-2133. doi:10.1101/gad.204401

Google Scholar: Author Only Title Only Author and Title

Sakuraba, Y., Kanno, S., Mabuchi, A, Monda, K., Iba, K., & Yanagisawa, S. (2018). A phytochrome-B-mediated regulatory mechanism of phosphorus acquisition. Nat Plants, 4(12), 1089-1101. doi:10.1038/s41477-018-0294-7

Google Scholar: Author Only Title Only Author and Title

Santos Teixeira, J. A, & Ten Tusscher, K. H. (2019). The Systems Biology of Lateral Root Formation: Connecting the Dots. Molecular Plant, 12(6), 784-803. doi:10.1016/j.molp.2019.03.015

Google Scholar: Author Only Title Only Author and Title

Satbhai, S. B., Setzer, C., Freynschlag, F., Slovak, R., Kerdaffrec, E., & Busch, W. (2017). Natural allelic variation of FRO2 modulates Arabidopsis root growth under iron deficiency. Nature Communications, 8, 15603. doi:10.1038/ncomms15603

Google Scholar: Author Only Title Only Author and Title

Scheet, P., & Stephens, M. (2006). A fast and flexible statistical model for large-scale population genotype data: applications to inferring missing genotypes and haplotypic phase. The American Journal of Human Genetics, 78(4), 629-644. doi:10.1086/502802

Google Scholar: Author Only Title Only Author and Title

Shahzad, Z., & Amtmann, A. (2017). Food for thought: how nutrients regulate root system architecture. Current Opinion in Plant Biology, 39, 80-87. doi:10.1016/j.pbi.2017.06.008

Google Scholar: Author Only Title Only Author and Title

Shani, E., Salehin, M., Zhang, Y., Sanchez, S. E., Doherty, C., Wang, R., . . . Estelle, M. (2017). Plant Stress Tolerance Requires Auxin-Sensitive Aux/IAA Transcriptional Repressors. Current Biology, 27(3), 437-444. doi:10.1016/j.cub.2016.12.016

Google Scholar: Author Only Title Only Author and Title

Shin, H., Shin, H. S., Dewbre, G. R., & Harrison, M. J. (2004). Phosphate transport in Arabidopsis: Pht1; 1 and Pht1; 4 play a major role in phosphate acquisition from both low-and high-phosphate environments. The Plant Journal, 39(4), 629-642. doi: 10.1111/j.1365-313X.2004.02161.x

Google Scholar: Author Only Title Only Author and Title

Spyropoulos IC, Liakopoulos TD, Bagos PG, Hamodrakas SJ. (2004) TMRPres2D: high quality visual representation of transmembrane protein models. Bioinformatics, 20(17), 3258-60. doi: 10.1093/bioinformatics/bth358.

Google Scholar: Author Only Title Only Author and Title

The UniProt Consortium (2017). UniProt: the universal protein knowledgebase. Nucleic Acids Research, 45(D1), D158-D169. doi:10.1093/nar/gkw1099

Google Scholar: Author Only Title Only Author and Title

Thorvaldsdottir, H., Robinson, J. T., & Mesirov, J. P. (2013). Integrative Genomics Viewer (IGV): high-performance genomics data visualization and exploration. Briefings in Bioinformatics, 14(2), 178-192. doi:10.1093/bib/bbs017

Google Scholar: Author Only Title Only Author and Title

Tusnady GE, Simon I. (2001) The HMMTOP transmembrane topology prediction server. Bioinformatics, 17(9), 849-50. doi: 10.1093/bioinformatics/17.9.849.

Google Scholar: Author Only Title Only Author and Title

Visscher, P. M., Wray, N. R., Zhang, Q., Sklar, P., McCarthy, M. I., Brown, M. A., & Yang, J. (2017). 10 Years of GWAS Discovery: Biology, Function, and Translation. The American Journal of Human Genetics, 101(1), 5-22. doi:https://doi.org/10.1016/j.ajhg.2017.06.005

Google Scholar: Author Only Title Only Author and Title

Ward, J. T., Lahner, B., Yakubova, E., Salt, D. E., & Raghothama, K. G. (2008). The effect of iron on the primary root elongation of Arabidopsis during phosphate deficiency. Plant Physiology, 147(3), 1181-1191. doi:10.1104/pp.108.118562

Google Scholar: Author Only Title Only Author and Title

Wolfe, D., Dudek, S., Ritchie, M. D., & Pendergrass, S. A. (2013). Visualizing genomic information across chromosomes with PhenoGram. BioData Min, 6(1), 18. doi:10.1186/1756-0381-6-18

Google Scholar: Author Only Title Only Author and Title

Wrolstad, R. E., Durst, R. W., & Lee, J. (2005). Tracking color and pigment changes in anthocyanin products. Trends in Food Science & Technology, 16(9), 423-428.

Google Scholar: Author Only Title Only Author and Title

Yin, H., Li, M., Lv, M., Hepworth, S. R., Li, D., Ma, C., . . . Wang, S. M. (2020). SAUR15 Promotes Lateral and Adventitious Root Development via Activating H(+)-ATPases and Auxin Biosynthesis. Plant Physiology, 184(2), 837-851. doi:10.1104/pp.19.01250

Google Scholar: Author Only Title Only Author and Title

Yu, J., Pressoir, G., Briggs, W. H., Bi, I. V., Yamasaki, M., Doebley, J. F., . . . Holland, J. B. (2006). A unified mixed-model method for association mapping that accounts for multiple levels of relatedness. Nature Genetics, 38(2), 203-208. doi: 10.1038/ng1702

Google Scholar: Author Only Title Only Author and Title

Yuan, H. M., Xu, H. H., Liu, W. C., & Lu, Y. T. (2013). Copper regulates primary root elongation through PIN1-mediated auxin redistribution. Plant and Cell Physiology, 54(5), 766-778. doi:10.1093/pcp/pct030

Google Scholar: Author Only Title Only Author and Title

Zmienko, A, Marszalek-Zenczak, M., Wojciechowski, P., Samelak-Czajka, A, Luczak, M., Kozlowski, P., . . . Figlerowicz, M. (2020). AthCNV: A Map of DNA Copy Number Variations in the Arabidopsis Genome. The Plant Cell, 32(6), 1797-1819. doi:10.1105/tpc.19.00640

Google Scholar: Author Only Title Only Author and Title